

Introduction to particle physics: experimental part

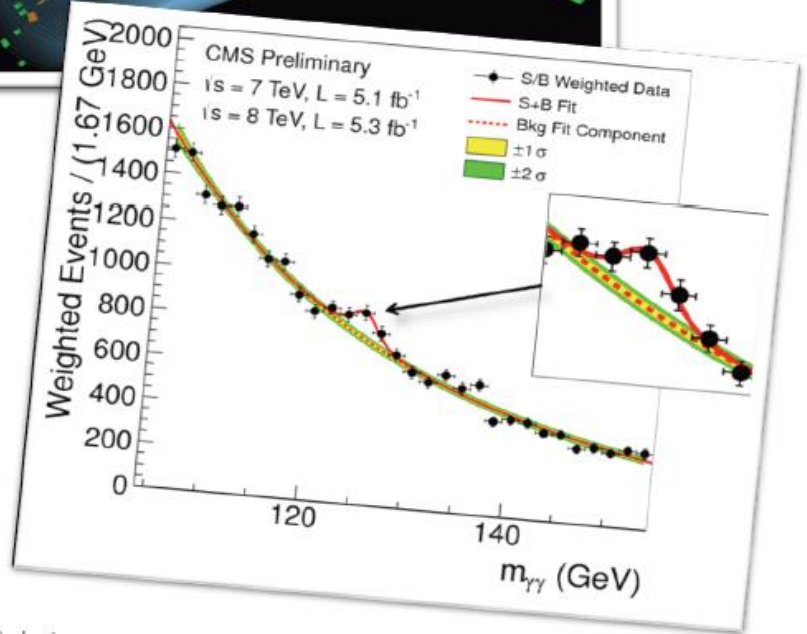
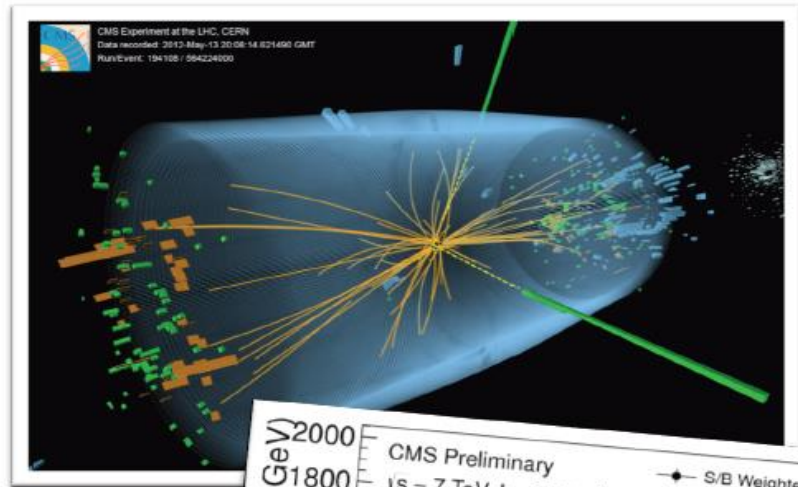
First data at LHC

Standard Model measurements

- **Soft and hard QCD**
- **b-jets**
- **W and Z bosons**
- **Prompt photons**
- **Top quarks**
- **Tau leptons**

Experiment = probing theories with data

$$\begin{aligned}
 & -\frac{1}{2}\partial_\nu g_\mu^\nu \partial_\nu g_\mu^\nu - g_s f^{abc} \partial_\nu g_\mu^\nu \partial_\nu g_\mu^\nu - \frac{1}{2}g_s^2 f^{abc} f^{ade} g_\mu^\nu g_\mu^\nu g_\mu^\nu g_\mu^\nu + \\
 & \frac{1}{2}g_s^2 (q_i^\mu \gamma^\mu q_j^\nu) g_\mu^\nu + G^a \partial^\mu G^a + g_s f^{abc} \partial_\mu G^a G^b G^c - \partial_\mu W_\nu^+ \partial_\mu W_\nu^- - \\
 & M^2 W_\mu^+ W_\mu^- - \frac{1}{2}\partial_\nu Z_\mu^0 \partial_\nu Z_\mu^0 - \frac{1}{2}g_s^2 M^2 Z_\mu^0 Z_\mu^0 - \frac{1}{2}\partial_\mu A_\nu \partial_\mu A_\nu - \frac{1}{2}\partial_\mu H \partial_\mu H - \\
 & \frac{1}{2}m_h^2 H^2 - \partial_\mu \phi^+ \partial_\mu \phi^- - M^2 \phi^+ \phi^- - \frac{1}{2}\partial_\nu \phi^\mu \partial_\nu \phi^\mu - \frac{1}{2}M \phi^\mu \phi^\mu - \beta_h \frac{[2M]^2}{2} + \\
 & 2M H + \frac{1}{2}(H^2 + \phi^\mu \phi^\mu + 2\phi^+ \phi^-) + \frac{2M^4}{\Lambda^2} \alpha_h - ig_{cw} [\partial_\nu Z_\mu^0 (W_\mu^+ W_\nu^- - \\
 & W_\mu^- W_\nu^+) - Z_\mu^0 (W_\nu^+ \partial_\nu W_\mu^- - W_\nu^- \partial_\nu W_\mu^+) + Z_\mu^0 (W_\nu^+ \partial_\nu W_\mu^- - \\
 & W_\nu^- \partial_\nu W_\mu^+) - ig_{sw} [\partial_\nu A_\mu (W_\mu^+ W_\nu^- - W_\mu^- W_\nu^+) - A_\nu (W_\mu^+ \partial_\mu W_\nu^- - \\
 & W_\mu^- \partial_\mu W_\nu^+) + A_\nu (W_\nu^+ \partial_\nu W_\mu^- - W_\nu^- \partial_\nu W_\mu^+) - \frac{1}{2}g^2 W_\mu^+ W_\mu^- W_\nu^+ W_\nu^- + \\
 & \frac{1}{2}g^2 W_\mu^+ W_\nu^- W_\mu^- W_\nu^+ + g^2 c_w^2 (Z_\mu^0 W_\mu^+ Z_\nu^0 W_\nu^- - Z_\mu^0 Z_\nu^0 W_\mu^+ W_\nu^-) + \\
 & g^2 s_w^2 (A_\mu W_\mu^+ A_\nu W_\nu^- - A_\mu A_\nu W_\mu^+ W_\nu^-) + g^2 s_w c_w [A_\mu Z_\nu^0 (W_\mu^+ W_\nu^- - \\
 & W_\mu^- W_\nu^+) - 2A_\mu Z_\nu^0 W_\mu^+ W_\nu^-] - g\alpha [H^2 + H\phi^\mu \phi^\mu + 2(\phi^\mu)^2 H^2] - \\
 & \frac{1}{8}g^2 \alpha_h [H^4 + (\phi^\mu)^4 + 4(\phi^\mu)^2 \phi^+ \phi^- + 4H^2 \phi^+ \phi^- + 2(\phi^\mu)^2 H^2] - \\
 & g M W_\mu^+ W_\nu^- H - \frac{1}{2}g \frac{M}{c_w} Z_\mu^0 Z_\nu^0 H - \frac{1}{2}ig [W_\mu^+ (H\partial_\nu \phi^- - \phi^- \partial_\nu H) - W_\mu^- (H\partial_\nu \phi^+ - \\
 & W_\nu^- (\phi^0 \partial_\nu \phi^+ - \phi^+ \partial_\nu \phi^0))] + \frac{1}{2}ig [W_\mu^+ (H\partial_\nu \phi^- - \phi^- \partial_\nu H) - W_\mu^- (H\partial_\nu \phi^+ - \\
 & \phi^+ \partial_\nu H)] + \frac{1}{2}g \frac{1}{c_w} (Z_\mu^0 (H\partial_\nu \phi^0 - \phi^0 \partial_\nu H) - ig_{cw}^2 M Z_\mu^0 (W_\mu^+ \phi^- - W_\mu^- \phi^+) + \\
 & ig_{sw} M A_\mu (W_\mu^+ \phi^- - W_\mu^- \phi^+) - ig \frac{1-2c_w^2}{2c_w} Z_\mu^0 (\phi^+ \partial_\nu \phi^- - \phi^- \partial_\nu \phi^+) - \\
 & ig_{sw} A_\mu (\phi^+ \partial_\nu \phi^- - \phi^- \partial_\nu \phi^+) - \frac{1}{2}g^2 W_\mu^+ W_\nu^- [H^2 + (\phi^\mu)^2 + 2\phi^+ \phi^-] - \\
 & ig_{sw} A_\mu (\phi^+ \partial_\nu \phi^- - \phi^- \partial_\nu \phi^+) + 2(2s_w^2 - 1)^2 \phi^+ \phi^- - \frac{1}{2}g^2 \frac{2c_w}{c_w} Z_\mu^0 \phi^\mu (W_\mu^+ \phi^- + \\
 & \frac{1}{4}g^2 \frac{1}{c_w} Z_\mu^0 Z_\nu^0 [H^2 + (\phi^\mu)^2 + 2(\phi^\mu)^2 \phi^+ \phi^-] + \frac{1}{2}g^2 s_w A_\mu \phi^\mu (W_\mu^+ \phi^- + \\
 & W_\mu^- \phi^+) - \frac{1}{2}ig^2 \frac{2c_w}{c_w} Z_\mu^0 H (W_\mu^+ \phi^- - W_\mu^- \phi^+) + \frac{1}{2}g^2 \frac{2c_w}{c_w} (2c_w^2 - 1) Z_\mu^0 A_\mu \phi^+ \phi^- - \\
 & W_\mu^+ \phi^+) + \frac{1}{2}ig^2 s_w A_\mu H (W_\mu^+ \phi^- - W_\mu^- \phi^+) - g^2 \frac{2c_w}{c_w} (2c_w^2 - 1) Z_\mu^0 A_\mu \phi^+ \phi^- - \\
 & g^2 s_w^2 A_\mu A_\nu \phi^+ \phi^- - e^\lambda (\gamma^\mu \partial^\nu e^\lambda - \partial^\lambda \gamma^\mu e^\lambda) - \rho^\lambda \gamma^\mu \partial^\nu \rho^\lambda - u_3^\lambda (\gamma^\mu \partial^\nu + m_\Delta^2) u_3^\lambda + \\
 & d_3^\lambda (\gamma^\mu \partial^\nu + m_\Delta^2) d_3^\lambda + ig_{sw} A_\mu [-(e^\lambda \gamma^\mu e^\lambda) + \frac{2}{3}(u_3^\lambda \gamma^\mu u_3^\lambda) - \frac{1}{3}(d_3^\lambda \gamma^\mu d_3^\lambda)] + \\
 & \frac{19}{4c_w} Z_\mu^0 [(\rho^\lambda \gamma^\mu (1 + \gamma^5) \nu^\lambda) + (e^\lambda \gamma^\mu (4s_w^2 - 1 - \gamma^5) e^\lambda) + (u_3^\lambda \gamma^\mu (\frac{2}{3}s_w^2 - \\
 & 1 - \gamma^5) u_3^\lambda) + (d_3^\lambda \gamma^\mu (1 - \frac{2}{3}s_w^2 - \gamma^5) d_3^\lambda)] + \frac{19}{2\sqrt{2}} W_\mu^+ [(\rho^\lambda \gamma^\mu (1 + \gamma^5) \nu^\lambda) + \\
 & (d_3^\lambda \gamma^\mu (1 + \gamma^5) C_{3\Delta} d_3^\lambda)] + \frac{19}{2\sqrt{2}} W_\mu^- [(e^\lambda \gamma^\mu (1 + \gamma^5) \nu^\lambda) + (d_3^\lambda \gamma^\mu (1 + \\
 & \gamma^5) u_3^\lambda)] + \frac{19}{2\sqrt{2}} \frac{m_\Delta^2}{M} [-\phi^+ (\nu^\lambda (1 - \gamma^5) e^\lambda) + \phi^- (e^\lambda (1 + \gamma^5) \nu^\lambda)] - \\
 & \frac{19}{2} \frac{m_\Delta^2}{M} [H (e^\lambda e^\lambda) + i\phi^0 (e^\lambda \gamma^5 e^\lambda)] + \frac{19}{2\sqrt{2}} \phi^+ [-m_\Delta^2 (u_3^\lambda C_{3\Delta} (1 - \gamma^5) d_3^\lambda) + \\
 & m_\Delta^2 (u_3^\lambda C_{3\Delta} (1 + \gamma^5) d_3^\lambda)] + \frac{19}{2\sqrt{2}} \phi^- [m_\Delta^2 (d_3^\lambda C_{3\Delta}^1 (1 + \gamma^5) u_3^\lambda) - m_\Delta^2 (d_3^\lambda C_{3\Delta}^1 (1 - \\
 & \gamma^5) u_3^\lambda)] - \frac{19}{2} \frac{m_\Delta^2}{M} H (u_3^\lambda u_3^\lambda) - \frac{19}{2} \frac{m_\Delta^2}{M} H (d_3^\lambda d_3^\lambda) + \frac{19}{2} \frac{m_\Delta^2}{M} \phi^0 (u_3^\lambda \gamma^5 u_3^\lambda) - \\
 & \frac{19}{2} \frac{m_\Delta^2}{M} \phi^0 (d_3^\lambda \gamma^5 d_3^\lambda) + X^+ (\partial^\mu - M^2) X^+ + X^- (\partial^\mu - M^2) X^- + X^0 (\partial^\mu - \\
 & \frac{M^2}{c_w} X^0 + \tilde{Y} \partial^\mu \tilde{Y} + ig_{cw} W_\mu^+ (\partial_\mu \tilde{X}^0 X^- - \partial_\mu \tilde{X}^+ X^0) + ig_{sw} W_\mu^+ (\partial_\mu \tilde{Y} X^- - \\
 & \partial_\mu \tilde{X}^+ Y) + ig_{cw} W_\mu^- (\partial_\mu \tilde{X}^- X^0 - \partial_\mu \tilde{X}^0 X^+) + ig_{sw} W_\mu^- (\partial_\mu \tilde{X}^- Y - \\
 & \partial_\mu \tilde{Y} X^+) + ig_{cw} Z_\mu^0 (\partial_\mu \tilde{X}^+ X^- - \partial_\mu \tilde{X}^- X^+) + ig_{sw} A_\mu (\partial_\mu \tilde{X}^+ X^- + \\
 & \partial_\mu \tilde{X}^- X^+) - \frac{1}{2}g M [\tilde{X}^+ X^+ H + \tilde{X}^- X^- H + \frac{1}{c_w} \tilde{X}^0 X^0 H] + \\
 & \frac{1-2c_w^2}{2c_w} ig M [\tilde{X}^+ X^0 \phi^+ - \tilde{X}^- X^0 \phi^-] + \frac{1}{2c_w} ig M [\tilde{X}^0 X^- \phi^+ - \tilde{X}^+ X^+ \phi^-] + \\
 & ig M s_w [\tilde{X}^0 X^- \phi^+ - \tilde{X}^+ X^+ \phi^-] + \frac{1}{2}ig M [\tilde{X}^+ X^+ \phi^0 - \tilde{X}^- X^- \phi^0]
 \end{aligned}$$



- Delamater

(experimental) LHC physics



- | | |
|----------------|--------------|
| Argentina | Morocco |
| Armenia | Netherlands |
| Australia | Norway |
| Austria | Poland |
| Azerbaijan | Portugal |
| Belarus | Romania |
| Brazil | Russia |
| Canada | Serbia |
| Chile | Slovakia |
| China | Slovenia |
| Colombia | South Africa |
| Czech Republic | Spain |
| Denmark | Sweden |
| France | Switzerland |
| Georgia | Taiwan |
| Germany | Turkey |
| Greece | UK |
| Israel | USA |
| Italy | CERN |
| Japan | JINR |

ATLAS Collaboration

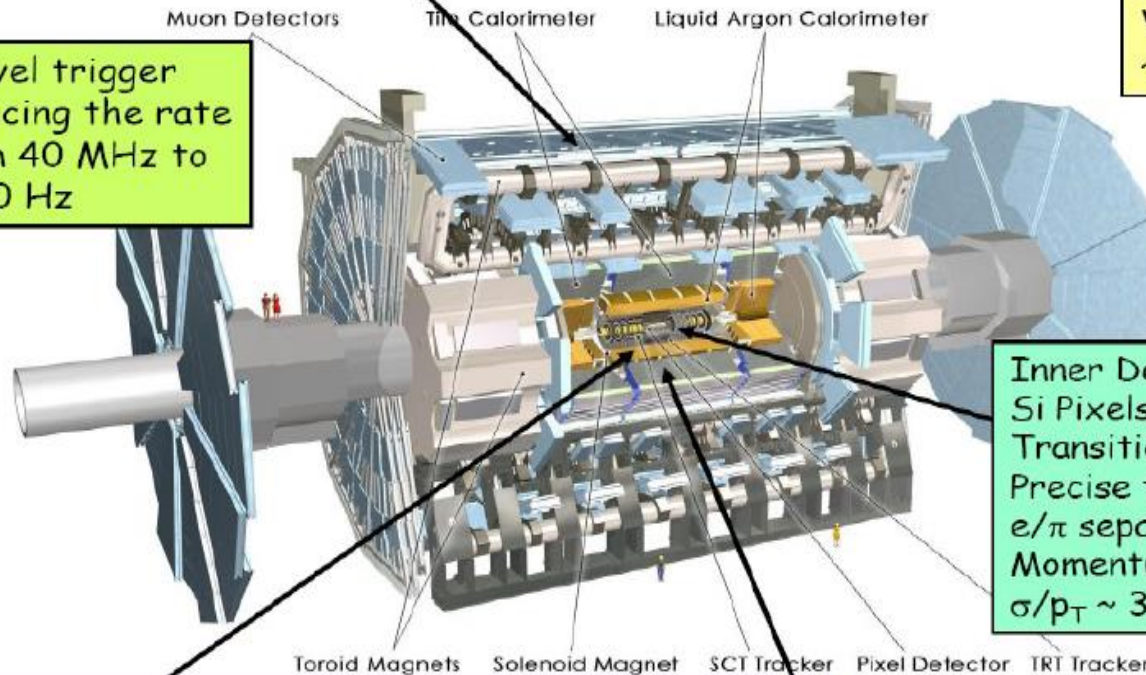


The ATLAS detector

Muon Spectrometer ($|\eta| < 2.7$): air-core toroids with gas-based chambers
 Muon trigger and measurement with momentum resolution $< 10\%$ up to $E_\mu \sim \text{TeV}$

Length : ~ 46 m
 Radius : ~ 12 m
 Weight : ~ 7000 tons
 $\sim 10^8$ electronic channels

3-level trigger
 reducing the rate
 from 40 MHz to
 ~ 200 Hz

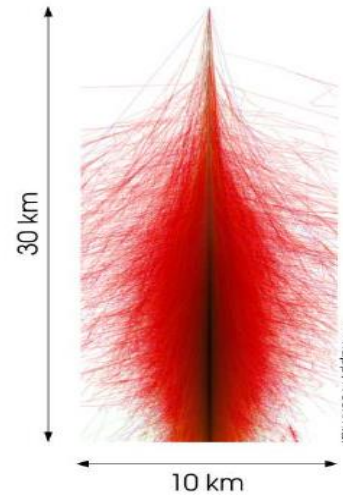
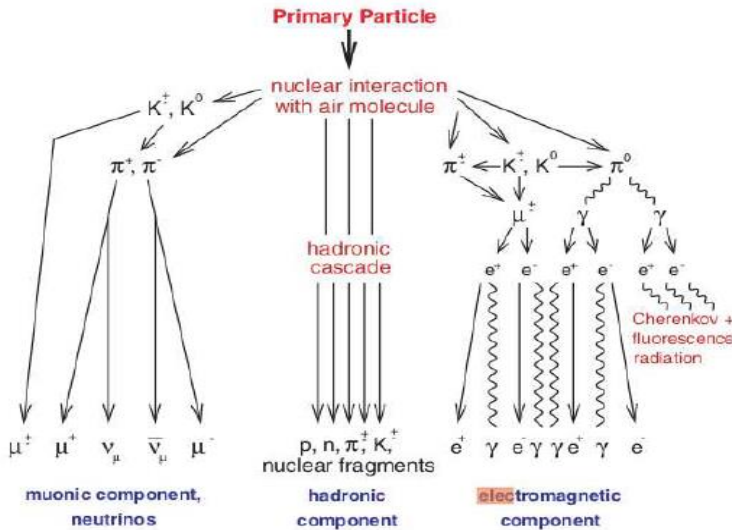


Inner Detector ($|\eta| < 2.5, B=2\text{T}$):
 Si Pixels and strips (SCT) +
 Transition Radiation straws
 Precise tracking and vertexing,
 e/π separation (TRT).
 Momentum resolution:
 $\sigma/p_T \sim 3.4 \times 10^{-4} p_T (\text{GeV}) \oplus 0.015$

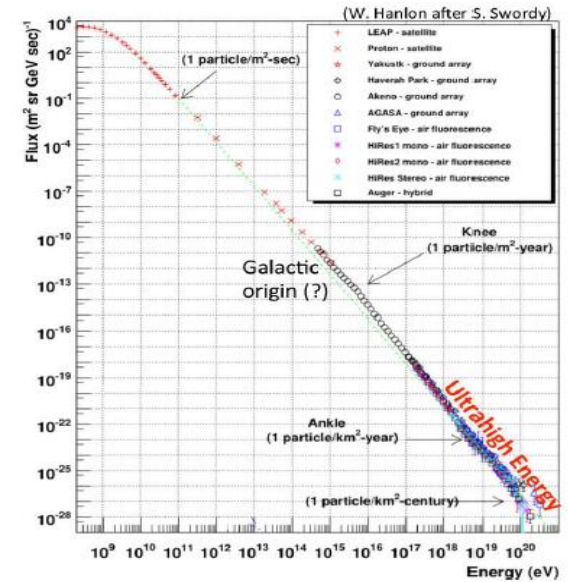
EM calorimeter: Pb-LAr Accordion
 e/γ trigger, identification and measurement
 E-resolution: $\sim 1\%$ at 100 GeV, 0.5% at 1 TeV

HAD calorimetry ($|\eta| < 5$): segmentation, hermeticity
 Tilecal Fe/scintillator (central), Cu/W-LAr (fwd)
 Trigger and measurement of jets and missing E_T
 E-resolution: $\sigma/E \sim 50\%/\sqrt{E} \oplus 0.03$

Cosmic rays



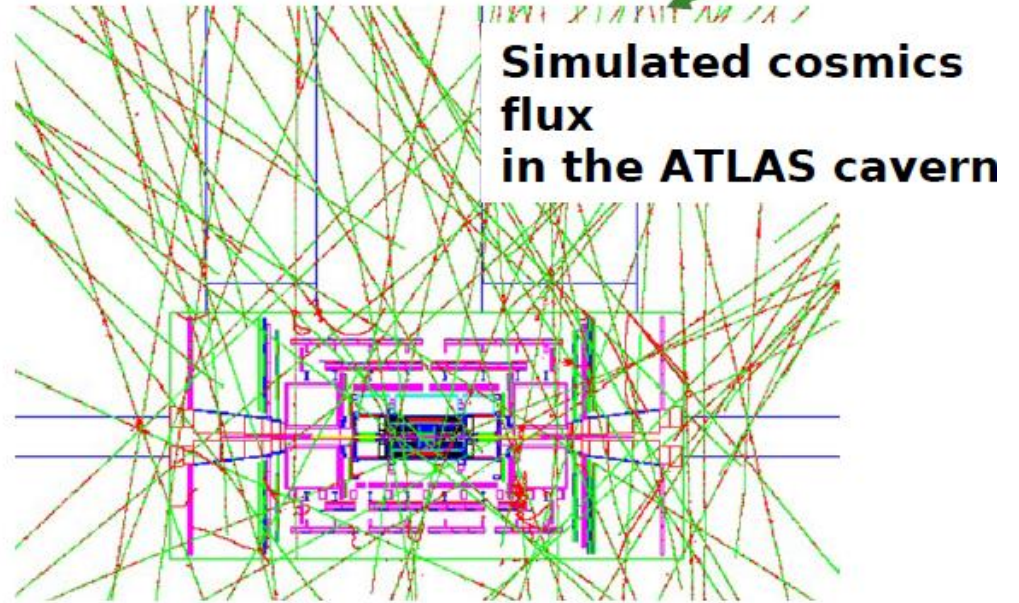
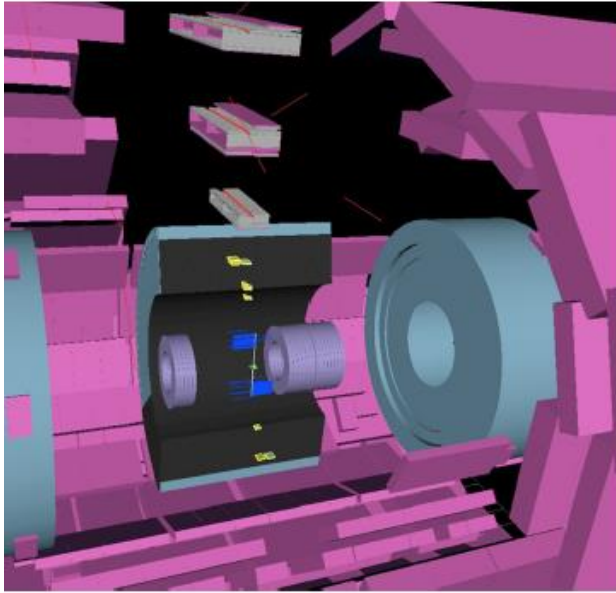
Simulation proton 10^{14} eV



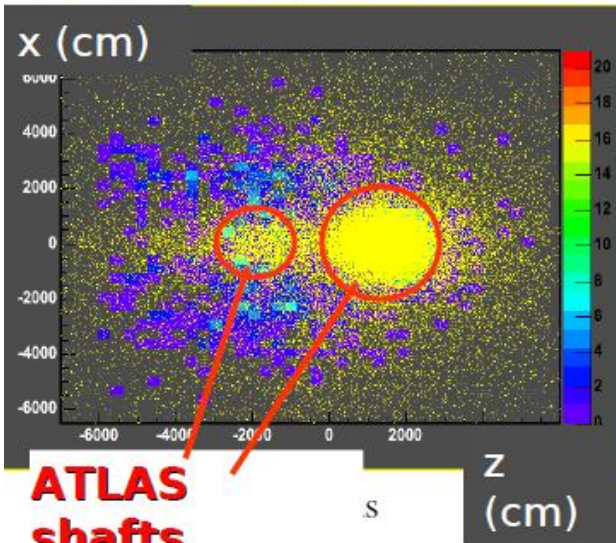
- The most penetrating component of atmospheric showers: the muon component
- At sea level muons represent about 80% of the cosmic ray flux
 - averaged over all energies
 - above $E \approx 1$ GeV they contribute almost 100%
- Below 1 GeV the energy spectrum of muons is almost flat
- Above 100 GeV falls exponentially
- It extends to extremely high energies
- The average cosmic ray muon energy is 4 GeV

Cosmic Muons in ATLAS

10 ms 2008



Real Cosmic Event



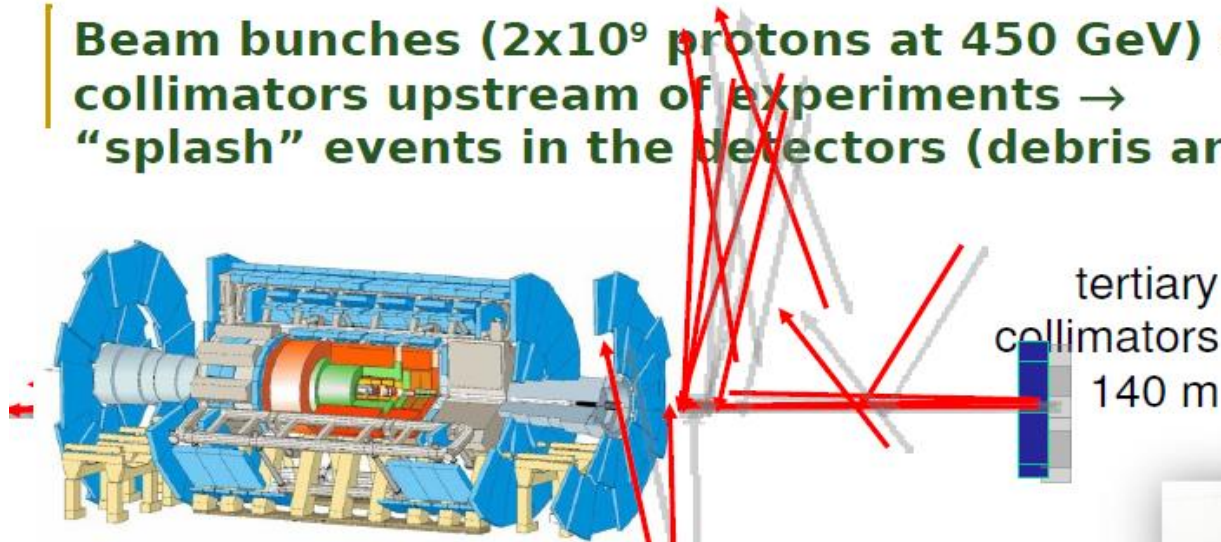
Muon impact points extrapolated to surface as measured by Muon Trigger chambers (RPC)

(Calorimeter trigger also

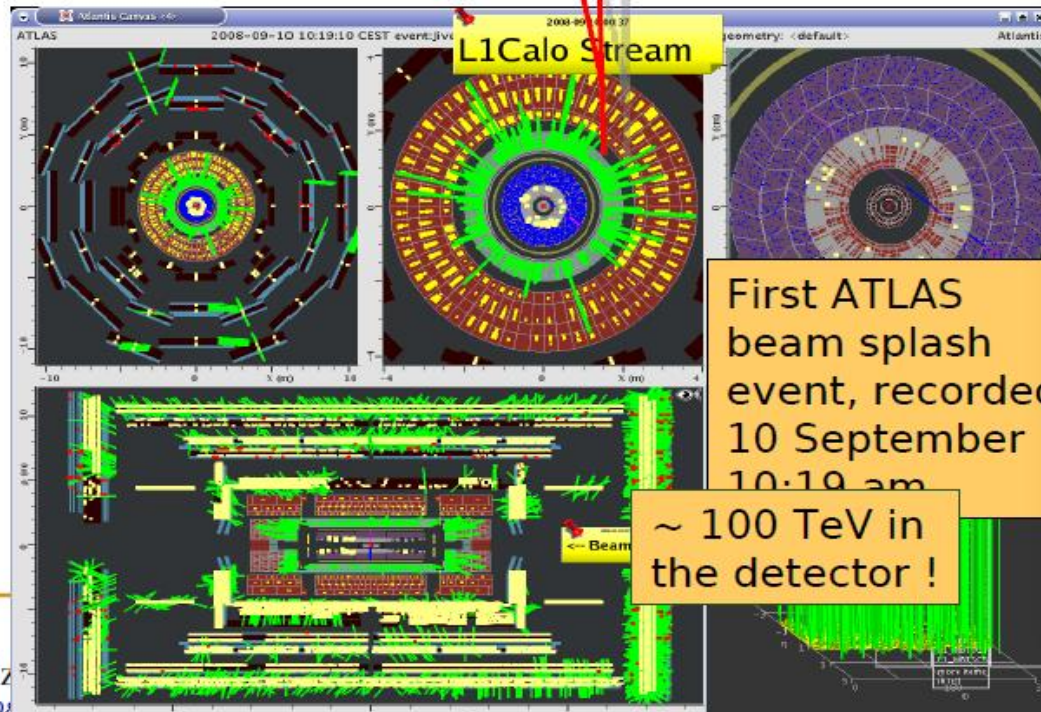
Rate ~100 m below ground:
~ 0(15 Hz) crossing Inner Detector



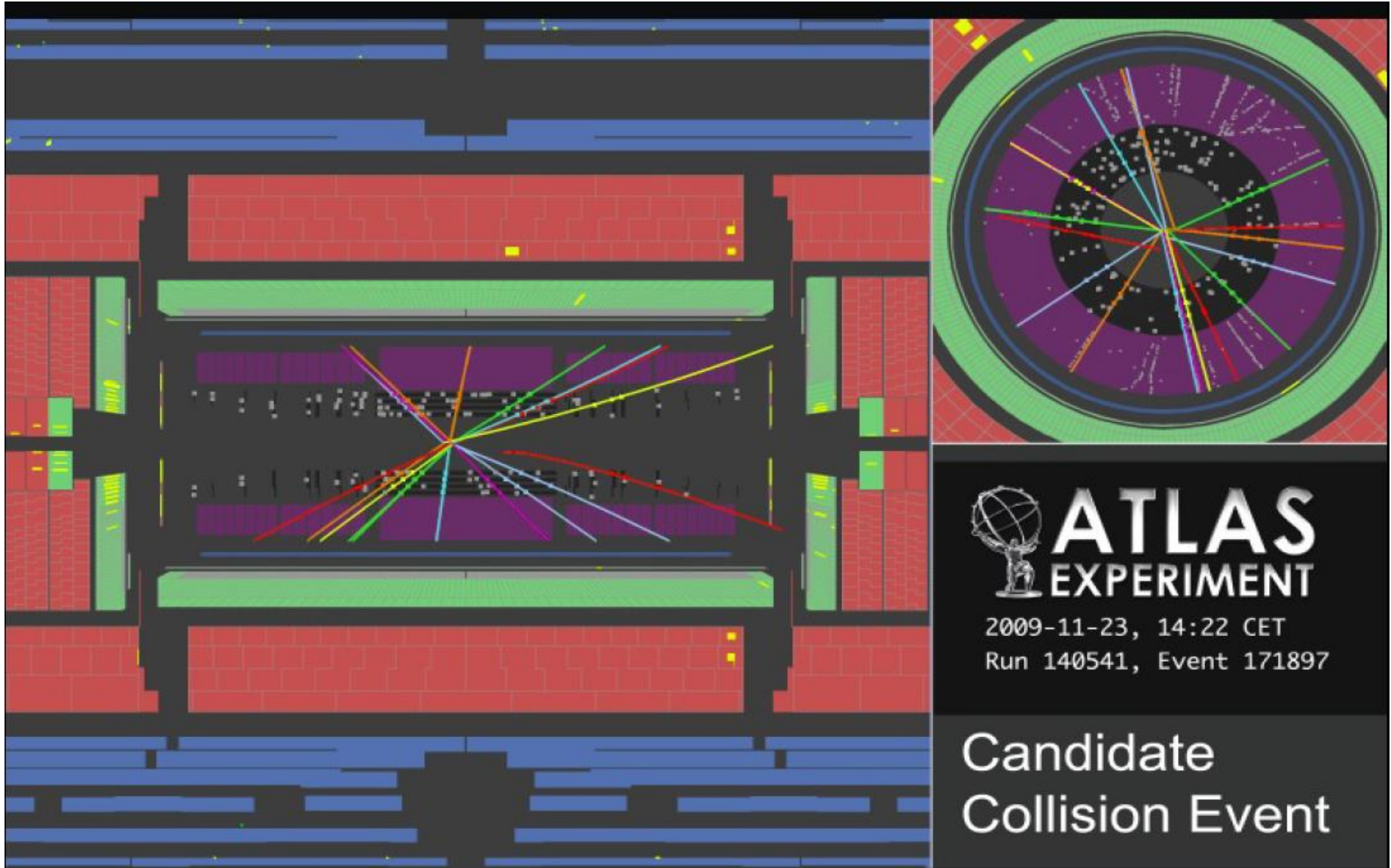
Beam bunches (2×10^9 protons at 450 GeV) stopped by (closed) collimators upstream of experiments \rightarrow "splash" events in the detectors (debris are mainly muons)



Beam pick-ups (BPT) (175 m)



First collisions in ATLAS (2009)

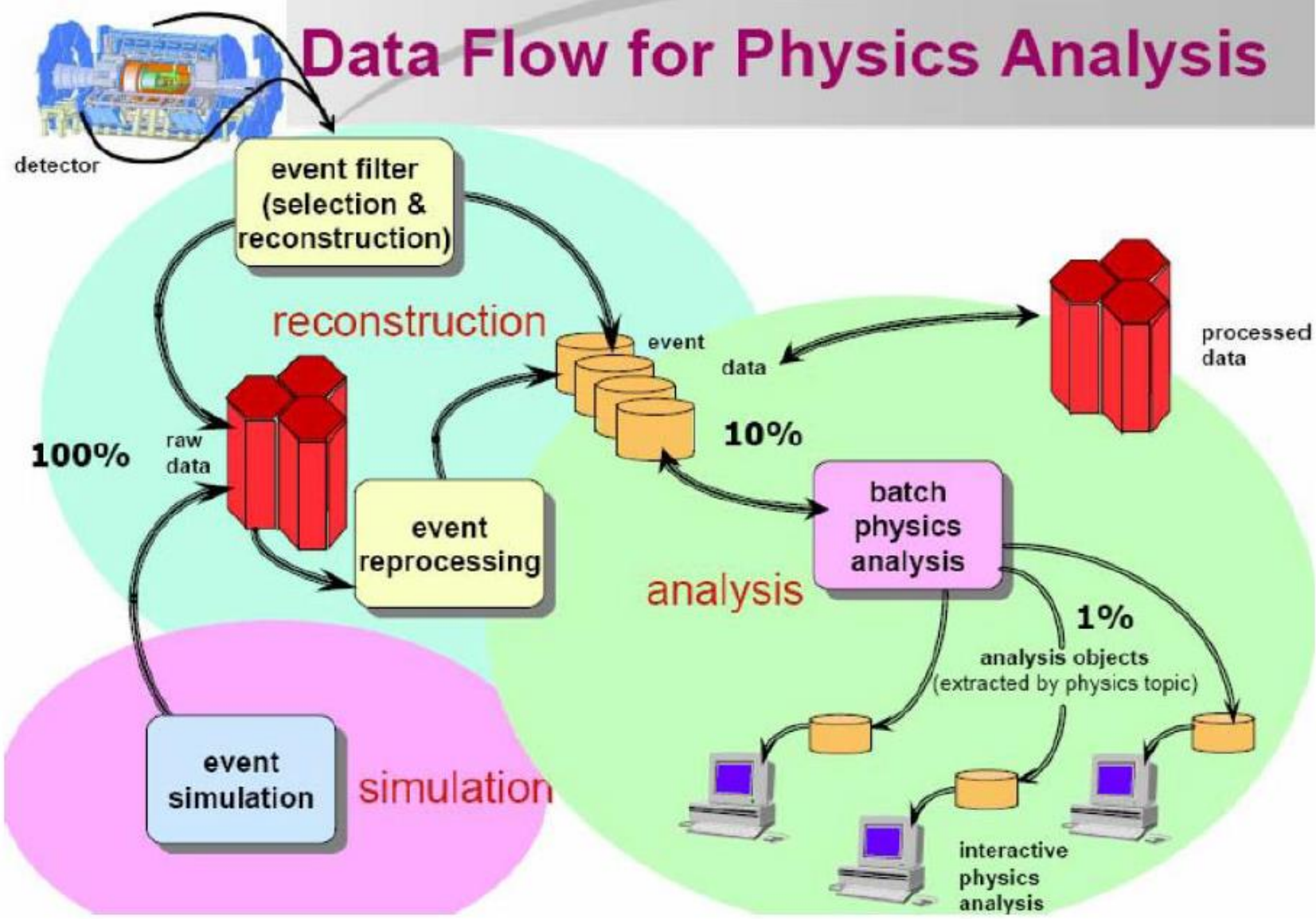


ATLAS
EXPERIMENT

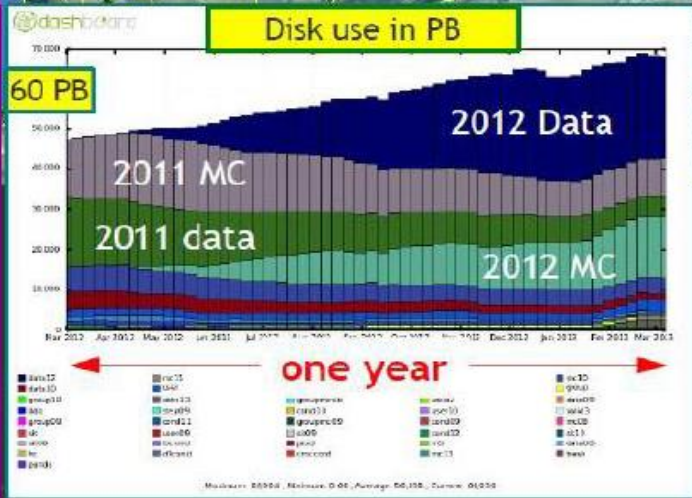
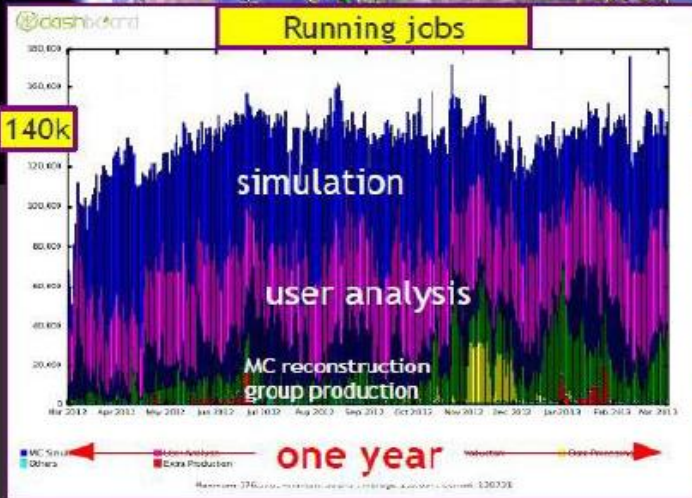
2009-11-23, 14:22 CET
Run 140541, Event 171897

Candidate
Collision Event

Data Flow for Physics Analysis



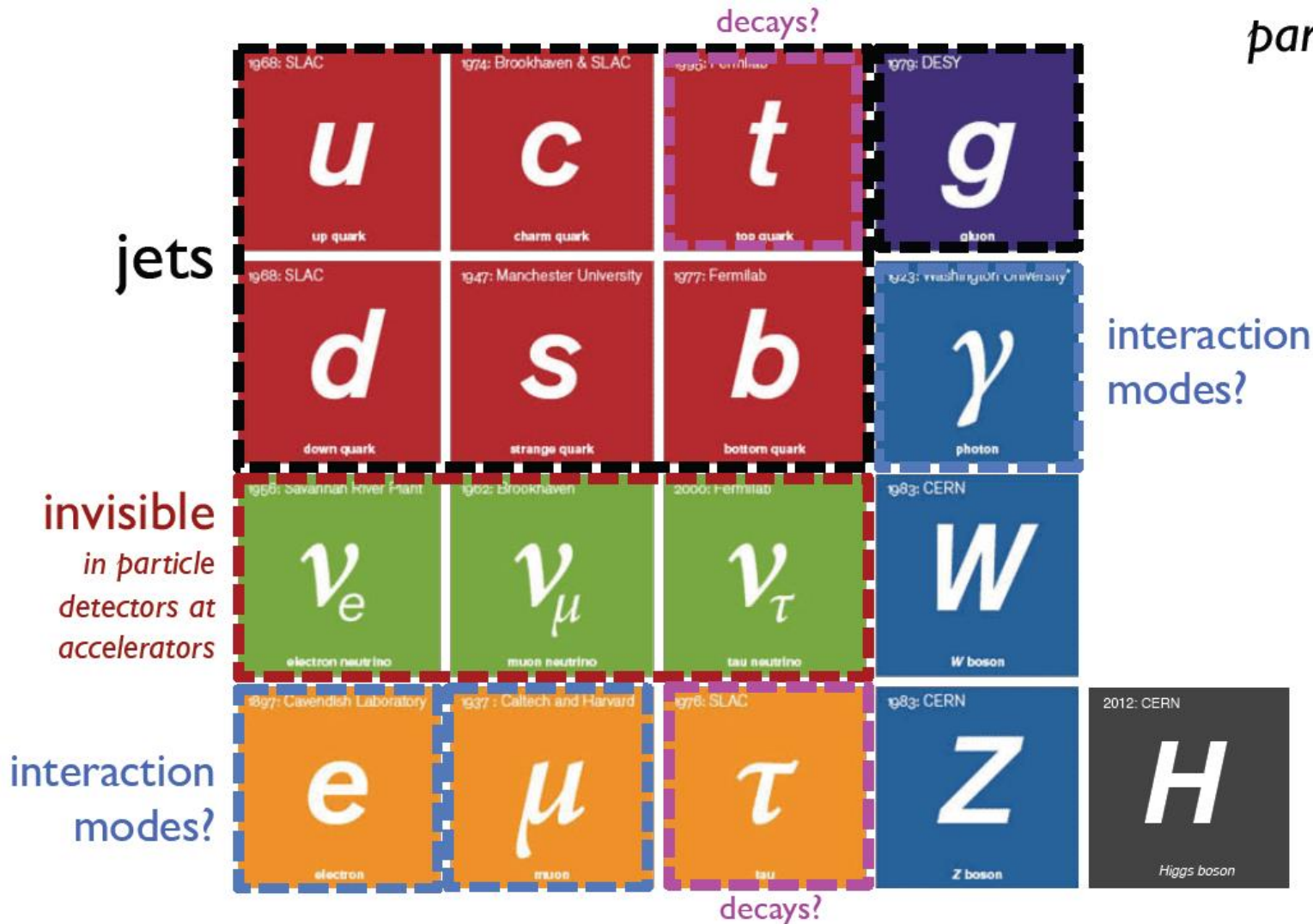
Worldwide LHC Computing Grid WLCG



ATLAS uses ~80
WLCG sites
world-wide
Performance is
superb

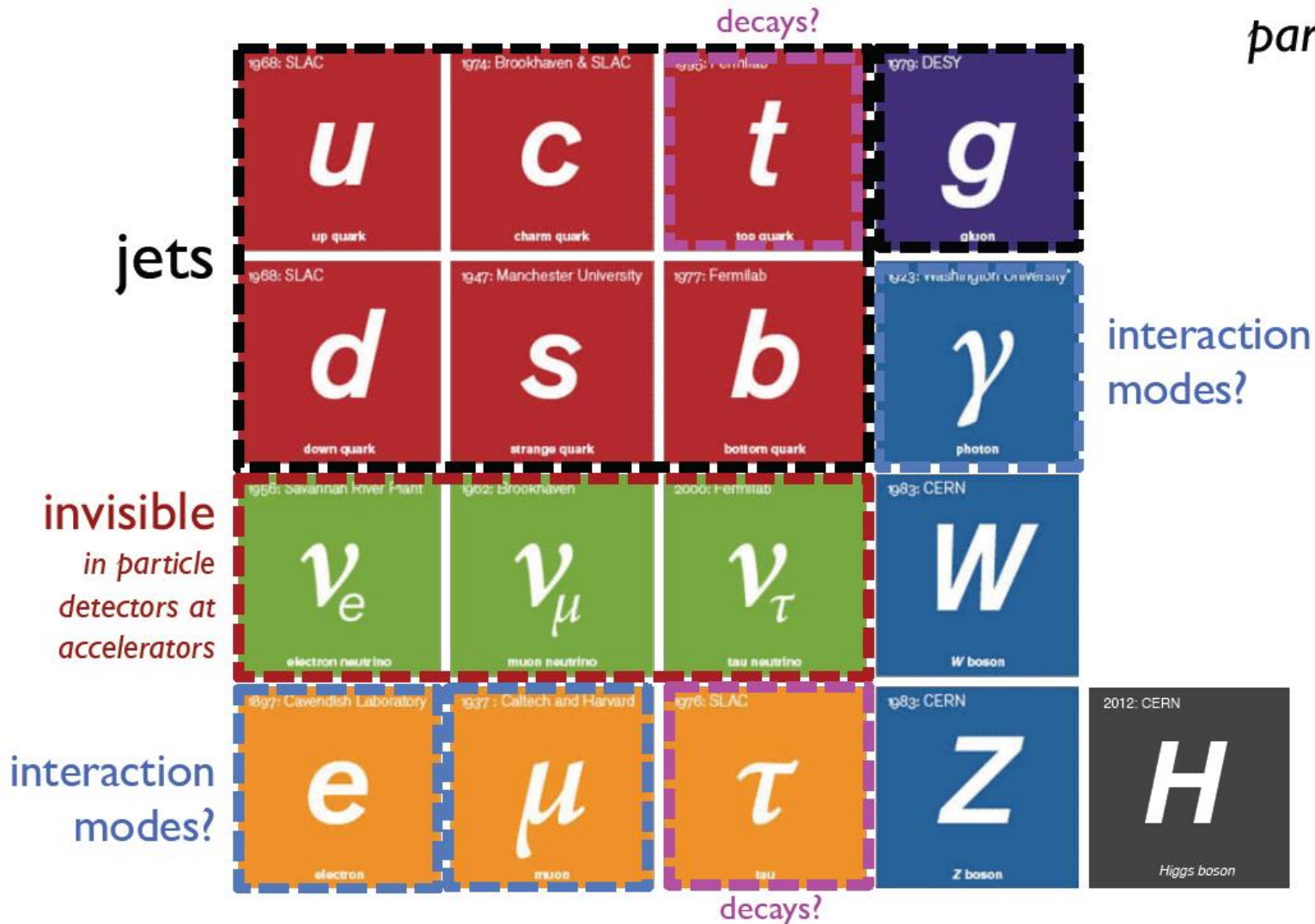
What do we want to measure?

... “stable”
particles!



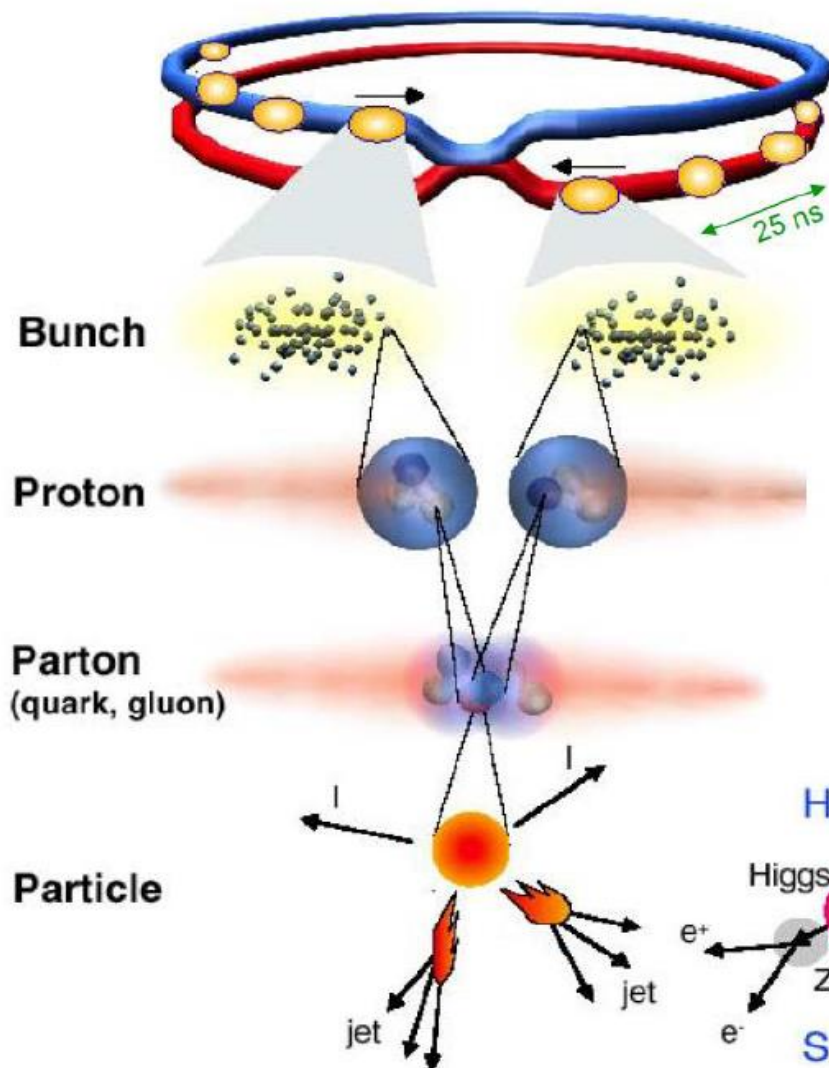
What do we want to measure?

... “stable”
particles!



Collisions at LHC

Proton-Proton	2835 bunch/beam
Protons/bunch	10^{11}
Beam energy	7 TeV (7×10^{12} eV)
Luminosity	10^{34} cm ⁻² s ⁻¹



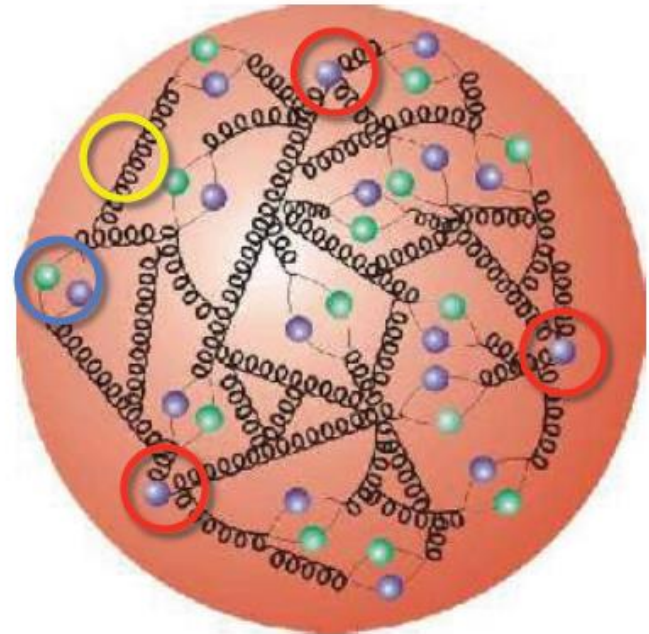
In the experiments:
 10^9 pp interactions per second
 ~ 1500 particles (p, n, π) produced in the detectors at each bunch-crossing

**Selection of 1 in
 10,000,000,000,000**

Inner structure of a proton

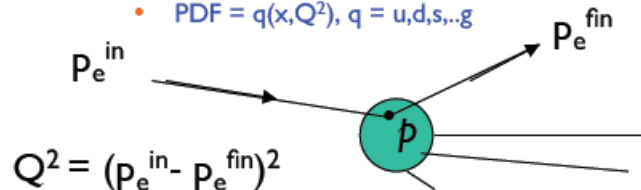
p protons have substructures

- ✓ partons = quarks & gluons
- ✓ 3 valence (colored) quarks bound by gluons
- ✓ Gluons (colored) have self-interactions
- ✓ Virtual quark pairs can pop-up (sea-quark)
- ✓ p momentum shared among constituents
 - described by p structure functions



Parton energy not 'monochromatic'

- ✓ Parton Distribution Function
 - PDF = $q(x, Q^2)$, $q = u, d, s, \dots, g$

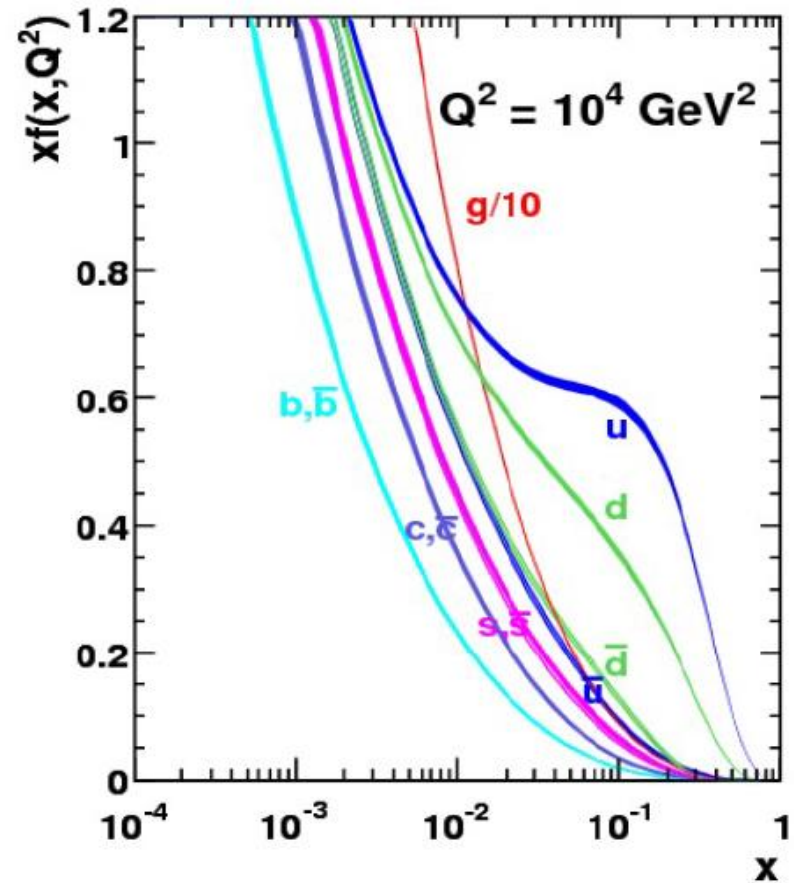
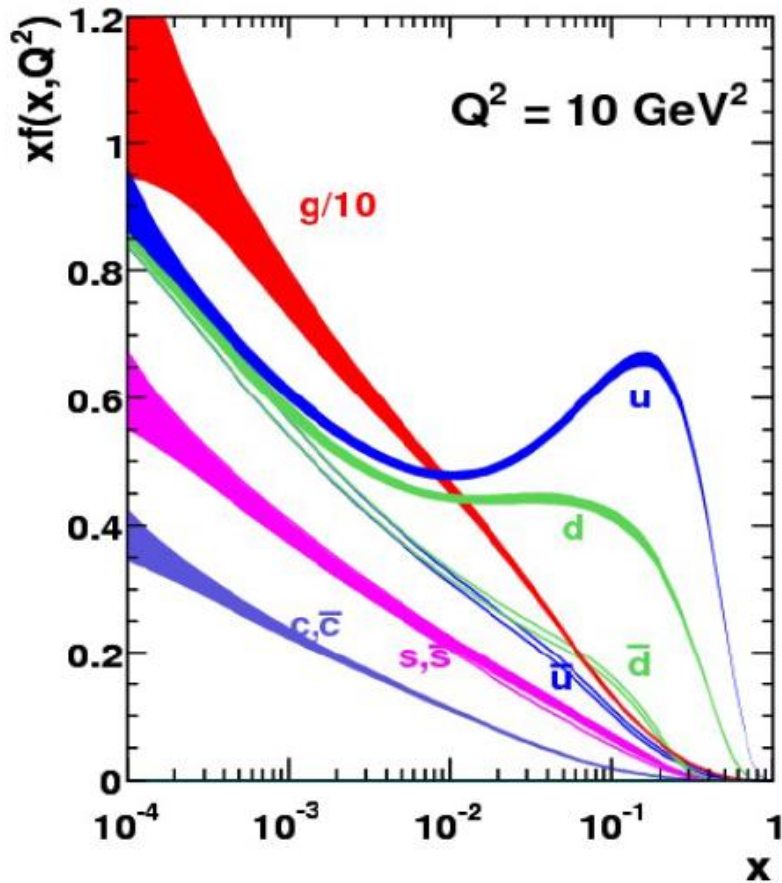


Kinematic variables

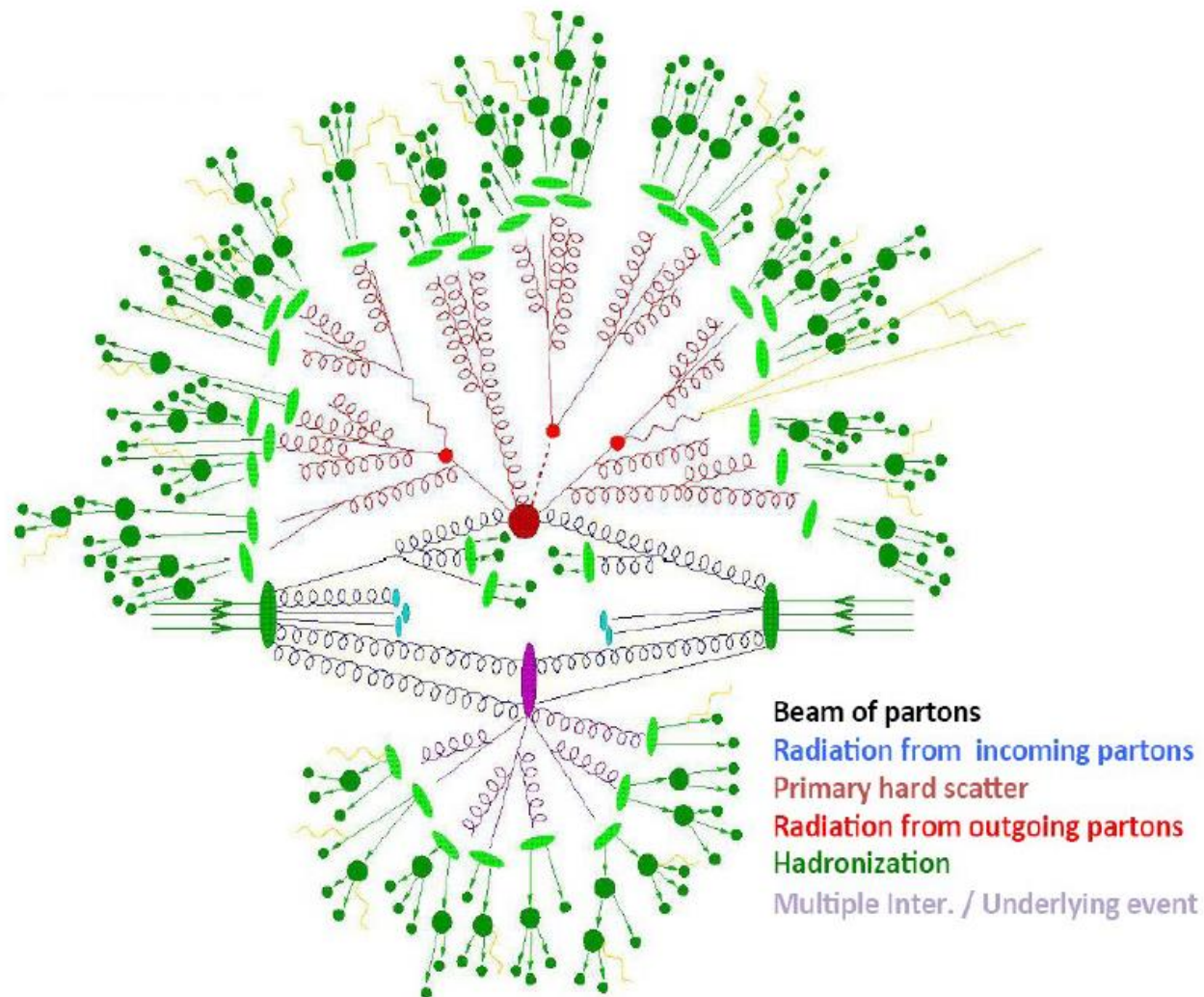
- ✓ Bjorken- x : fraction of the proton momentum carried by struck parton
 - $x = P_{parton} / P_{proton}$
- ✓ Q^2 : 4-momentum² transfer

Inner structure of a proton

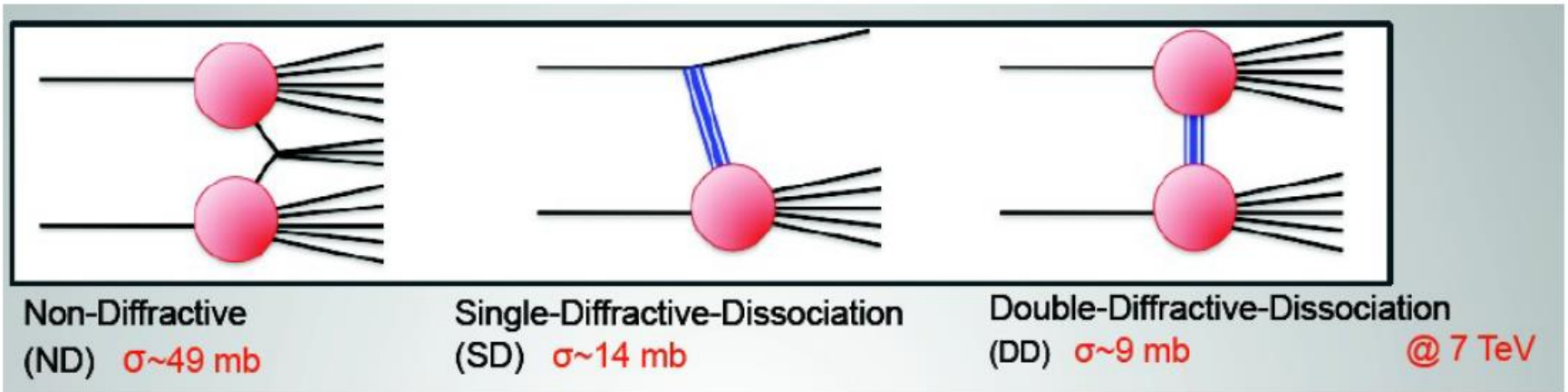
MSTW 2008 NLO PDFs (68% C.L.)



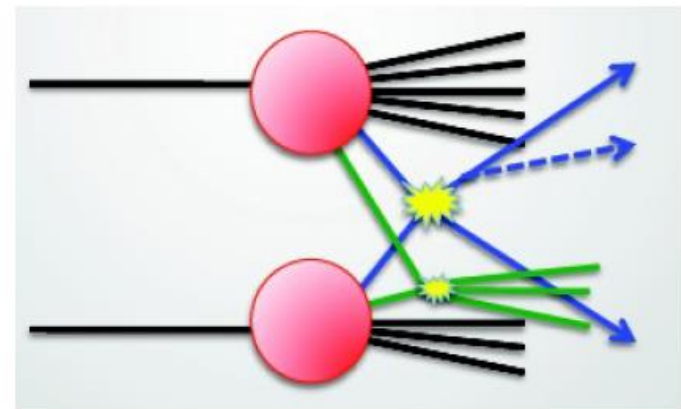
Monte Carlo model for typical pp collision



Dominant QCD processes



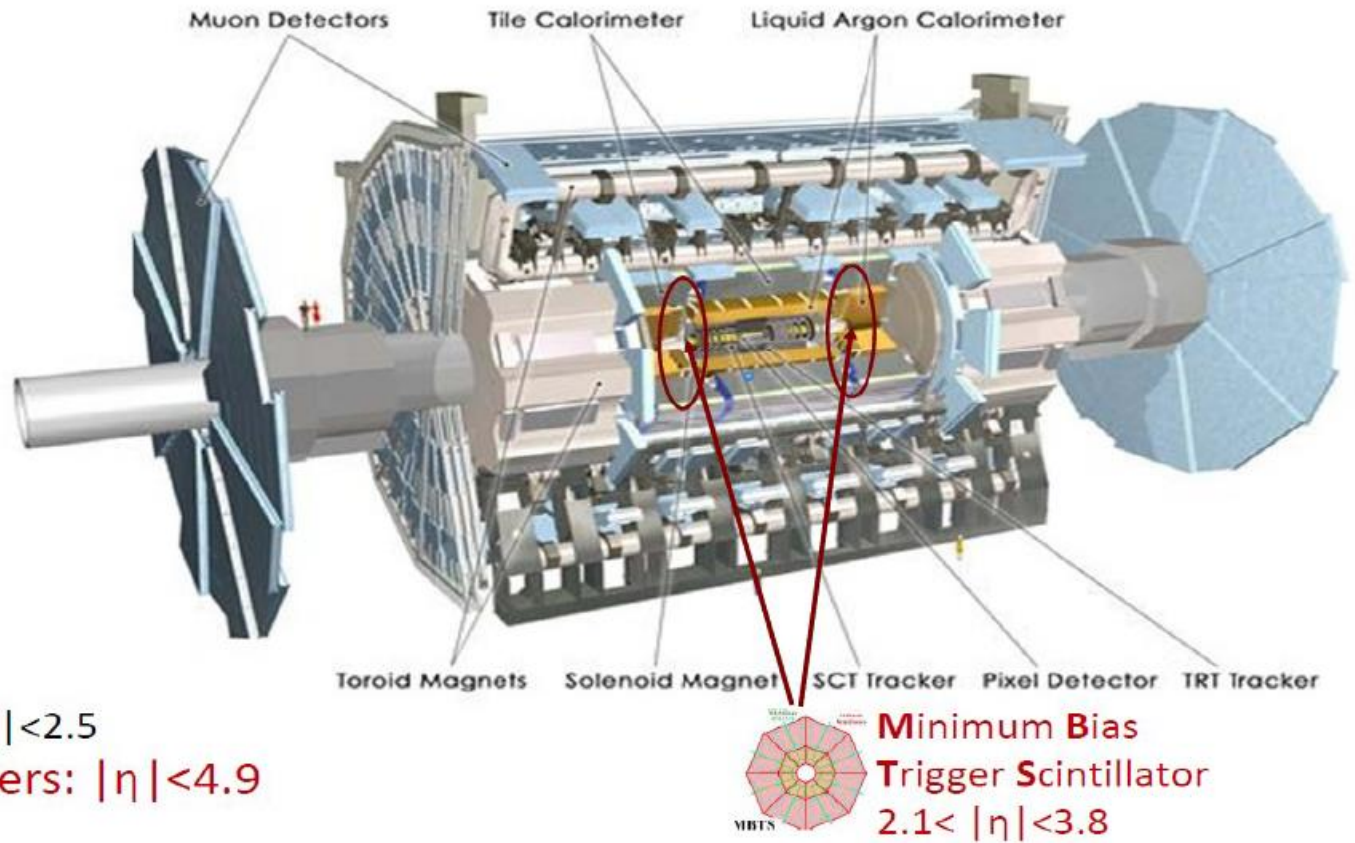
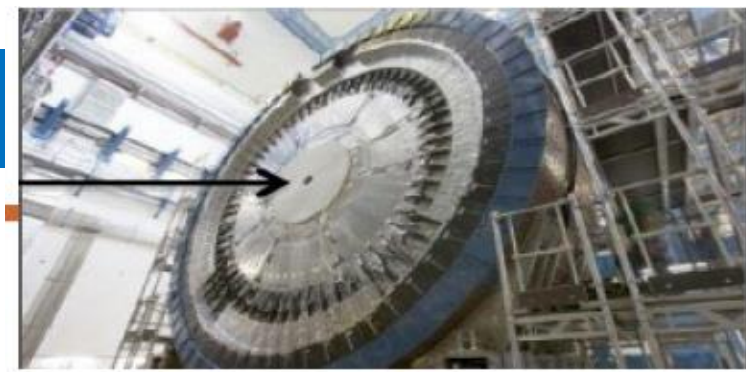
- Multi-parton interactions (**Underlying Event**)



Inelastic cross-sections

- Use only few runs: 7 TeV data ($190 \mu\text{b}^{-1}$) + 900 GeV data ($7 \mu\text{b}^{-1}$) and 2.36 TeV data ($0.1 \mu\text{b}^{-1}$)
 - We want to study **all** inelastic pp interactions
 - Instantaneous luminosity very low for these runs: on average ~ 0.007 interactions per bunch crossing \rightarrow **99.3% of crossings are empty.**
 - Need to **“trigger”** on inelastic interactions:
Minimum Bias Scintillator Trigger (MBTS)
 - \rightarrow sensitive to any charged particle $2.09 < |\eta| < 3.84$
 - \rightarrow 16 counters on each side of ATLAS
- Correct for detector inefficiencies and resolution, eg. present **spectrum of charge particles** not tracks
- **No extrapolation** to regions not seen by ATLAS

MBST Trigger

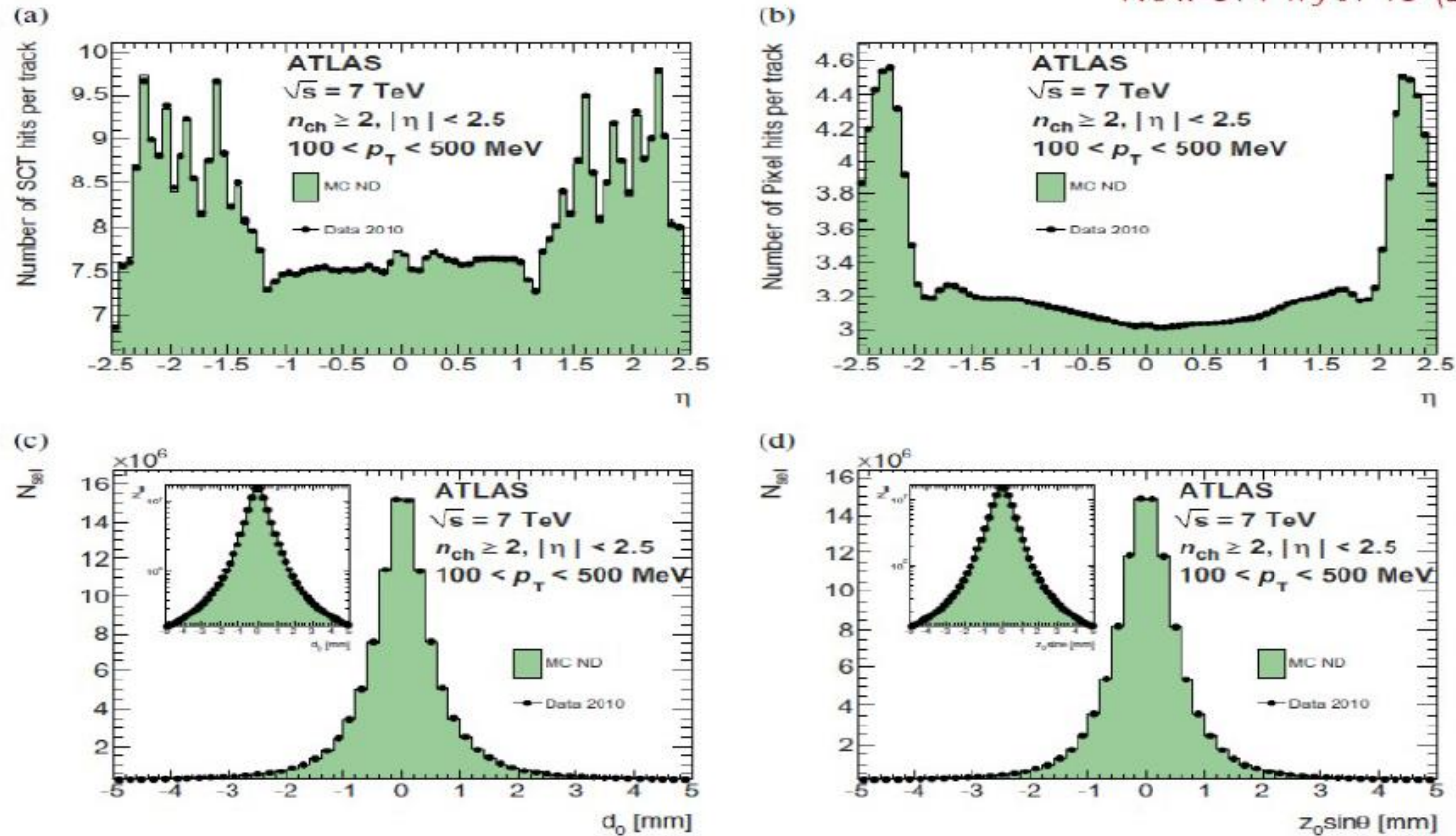


Trackers: $|\eta| < 2.5$

Calorimeters: $|\eta| < 4.9$

How well we understood detector?

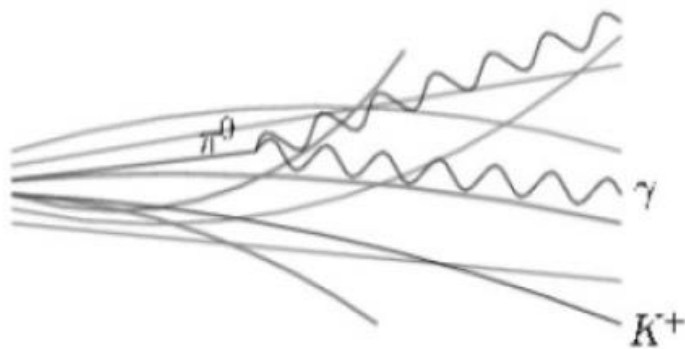
New J. Phys. 13 (2011) 053033



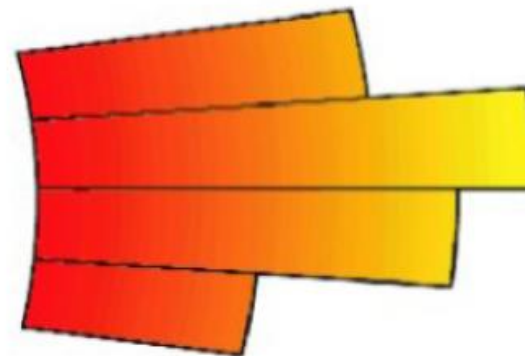
- Excellent agreement between data and MC: Pixel and Silicon hits per track

Unfolding to particle level

- Bayesian iterative unfolding used to correct tracks and clusters back to particle level.
 - Use mapping of truth particles on reconstructed objects (use Monte Carlo)



particle level

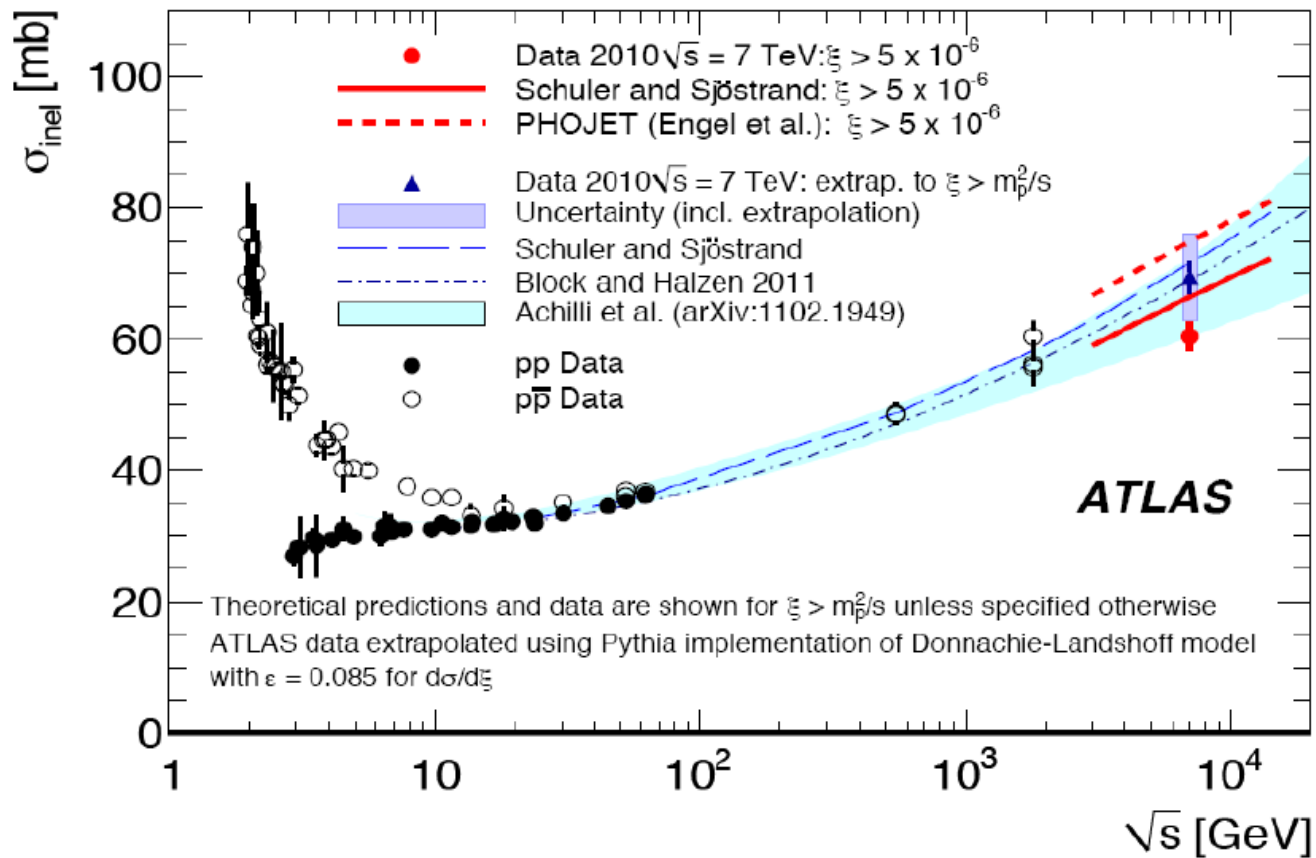


detector level

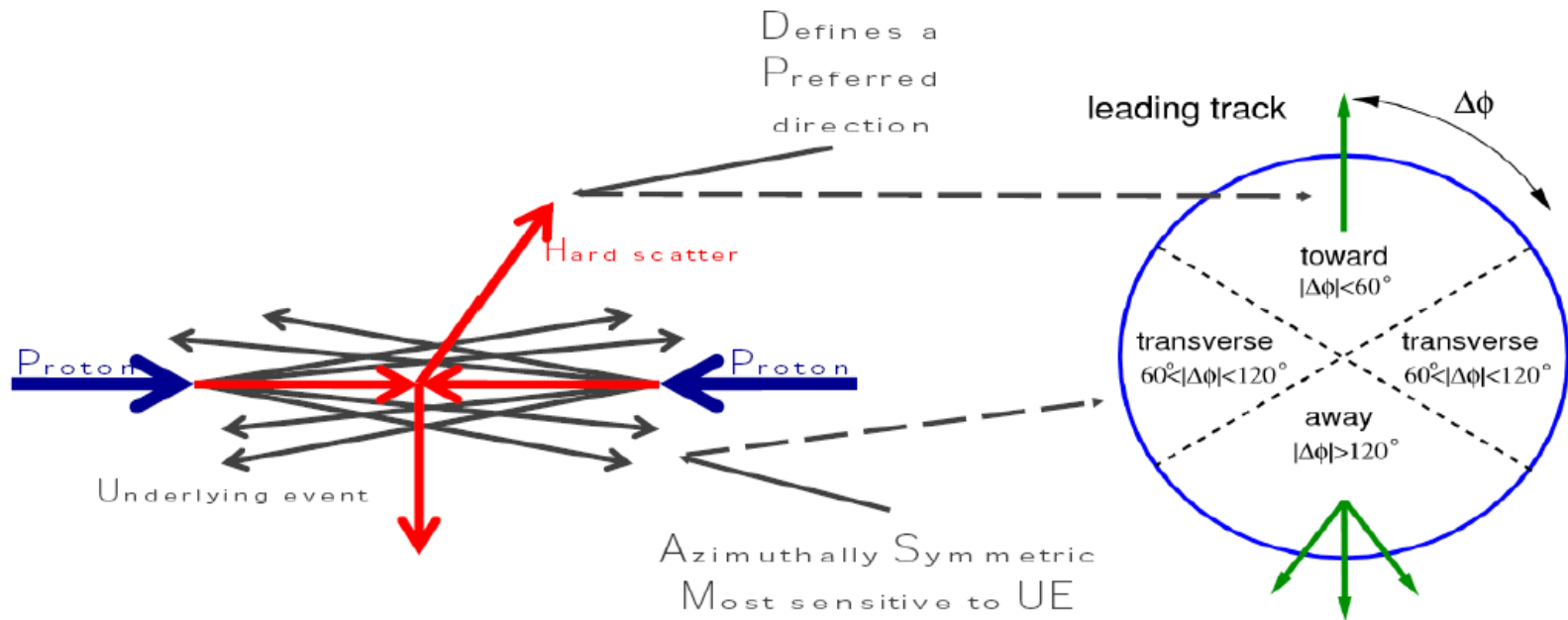
Total inelastic cross-section

$$\sigma(\xi > 5 \cdot 10^{-6}) = 60.3 \pm 0.05 \text{ (stat.)} \pm 0.5 \text{ (sys.)} \pm 2.1 \text{ (lumi) mb}$$

$$\sigma_{inel} = 69.1 \pm 2.4 \text{ (exp.)} \pm 6.9 \text{ (extr.) mb}$$

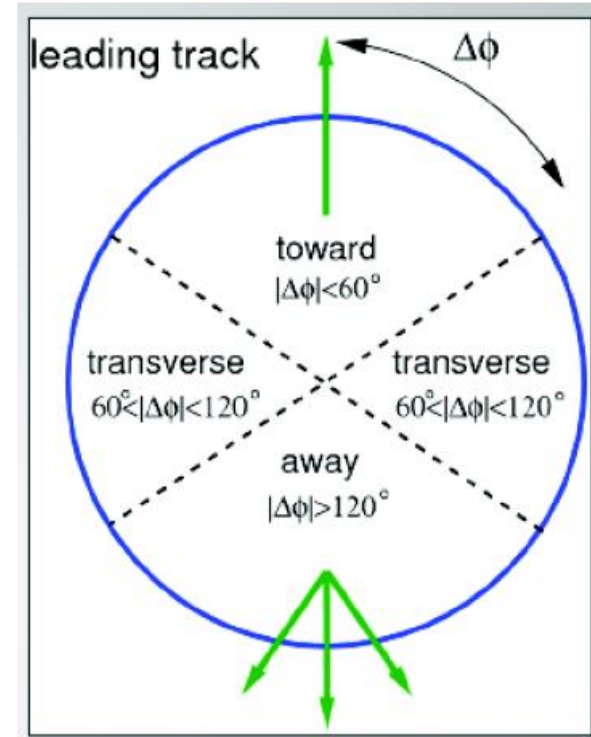
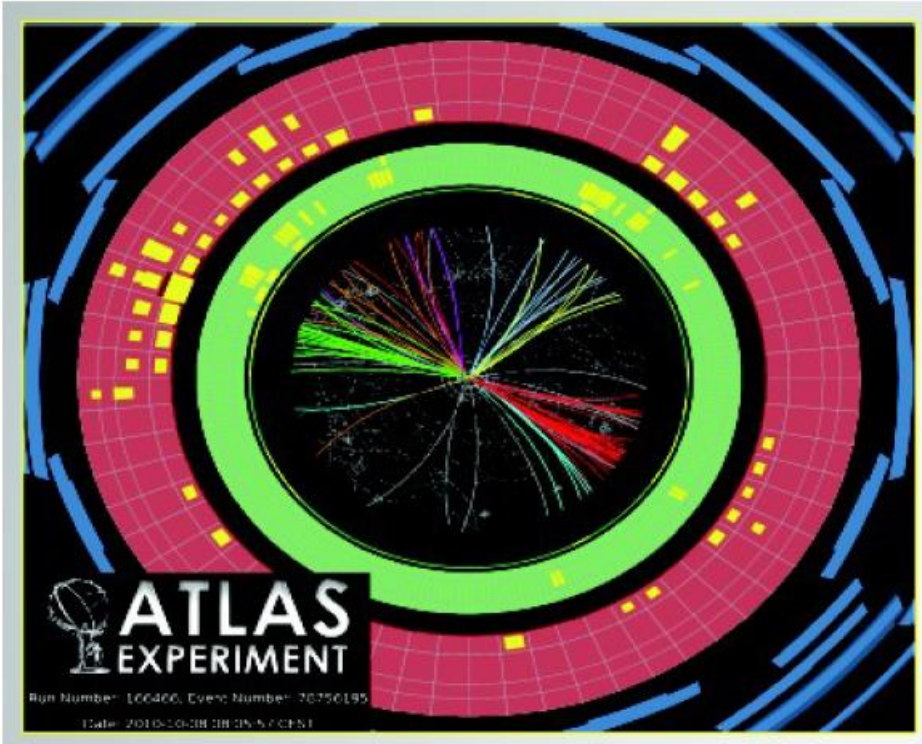


Underlying event



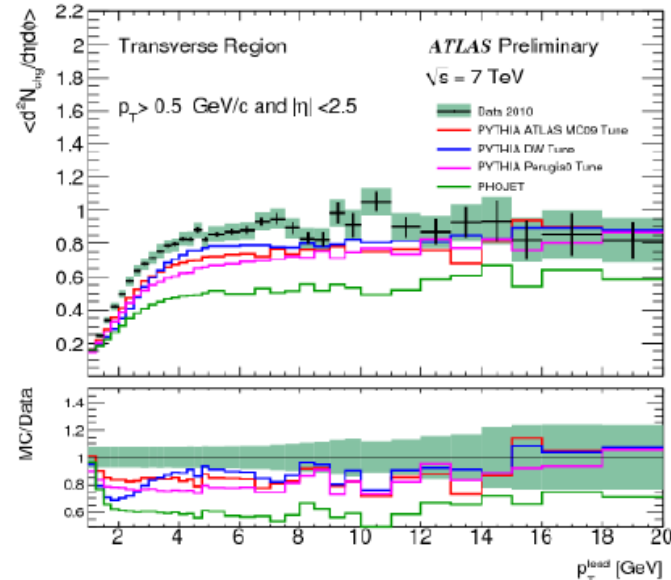
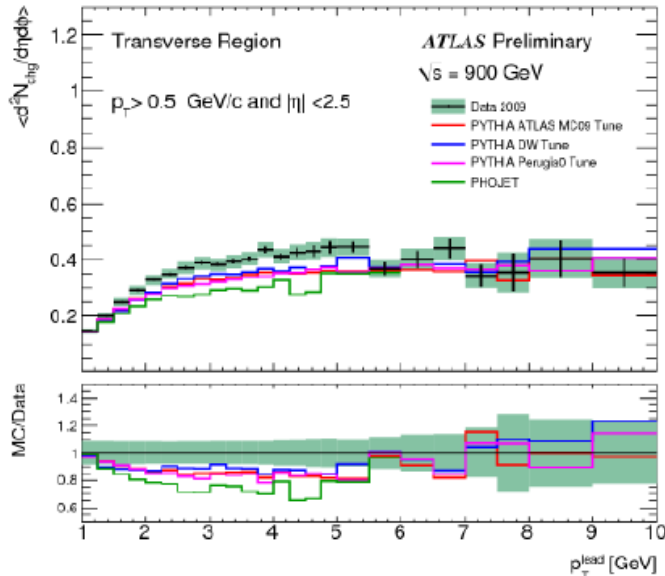
- UE = “everything” - “hard scatter” = beam-beam remnants, MPI, ISR
- Study: charged particle density, transverse momentum, average p_T . Transverse region considered most sensitive to UE

Underlying event



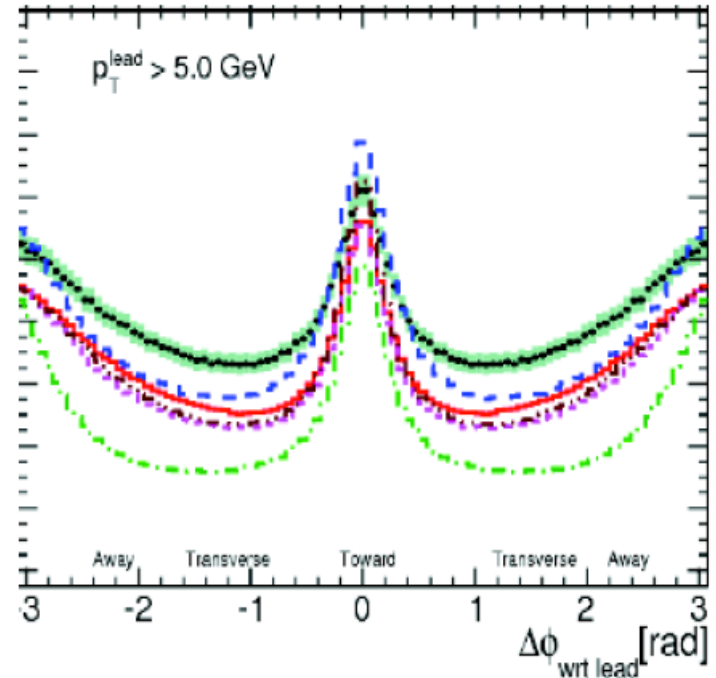
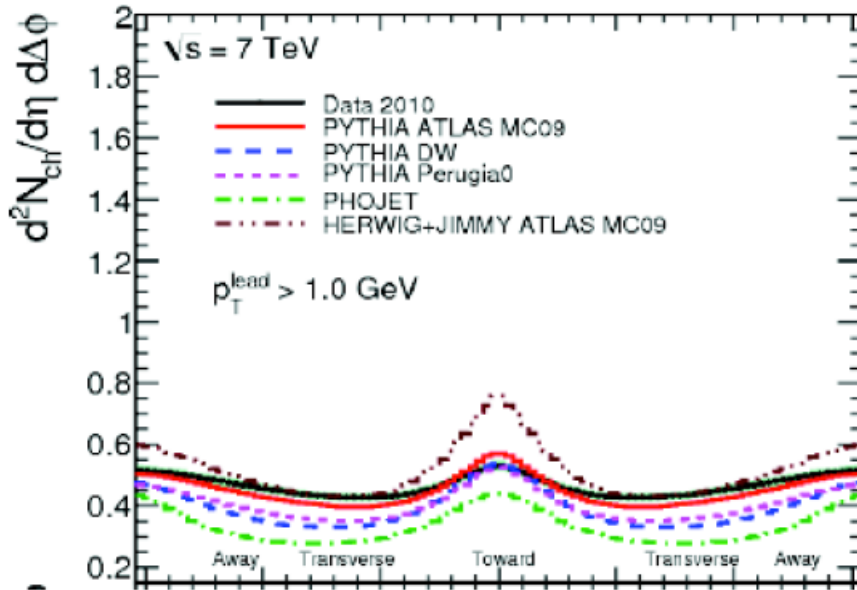
- Define the direction of “hard scatter” as the highest p_T particle
- Study the activity (#of particles) in the region “transverse” to the hard scatter.

Transverse region particle density



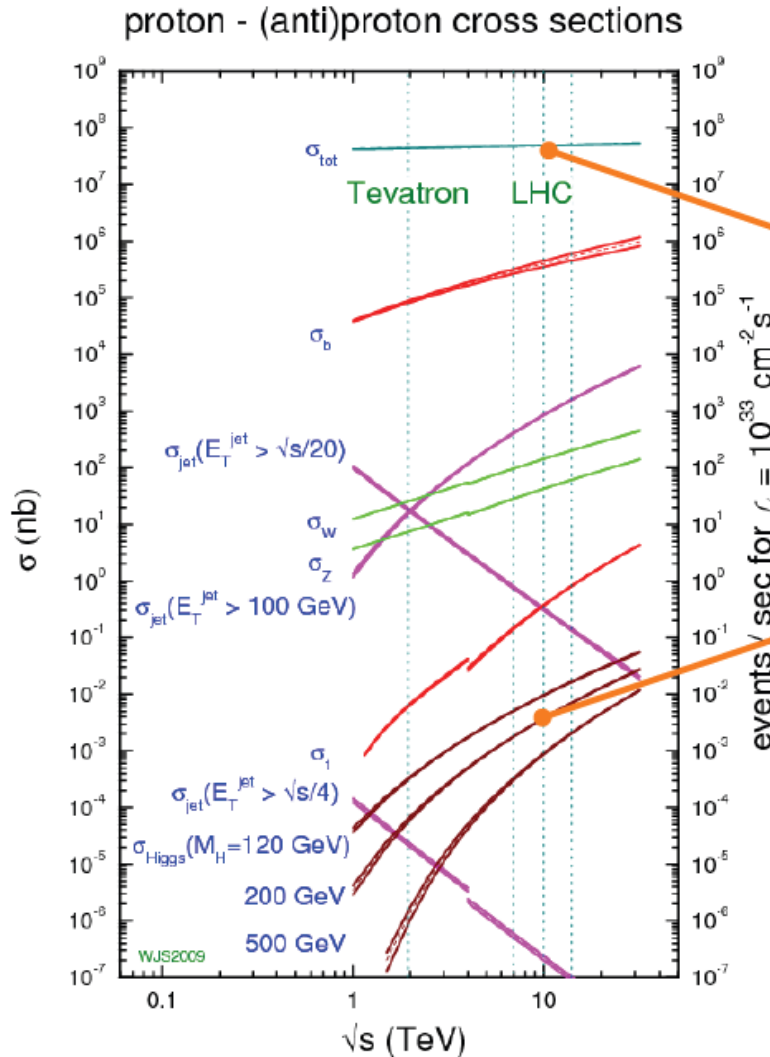
- All tunes underestimate particle density by 10%-15% in the plateau region
- There is factor of ~ 2 increase in activities between 900 GeV and 7 TeV
- In the plateau region the measured density corresponds to ~ 2.5 per unit η at 900 GeV and 5 particle at 7 TeV

Particle density angular correlations



- Define the event orientation by the azimuthal angle on the track with the highest p_T .
- MC tunes only reproduce the general features, disagreement in rates both in the transverse region (UE) and in the away region (MPI/Hard Core)

Cross-sections at LHC



10^8 events/s

$\sim 10^{10}$

10^{-2} events/s \sim

10 events/min

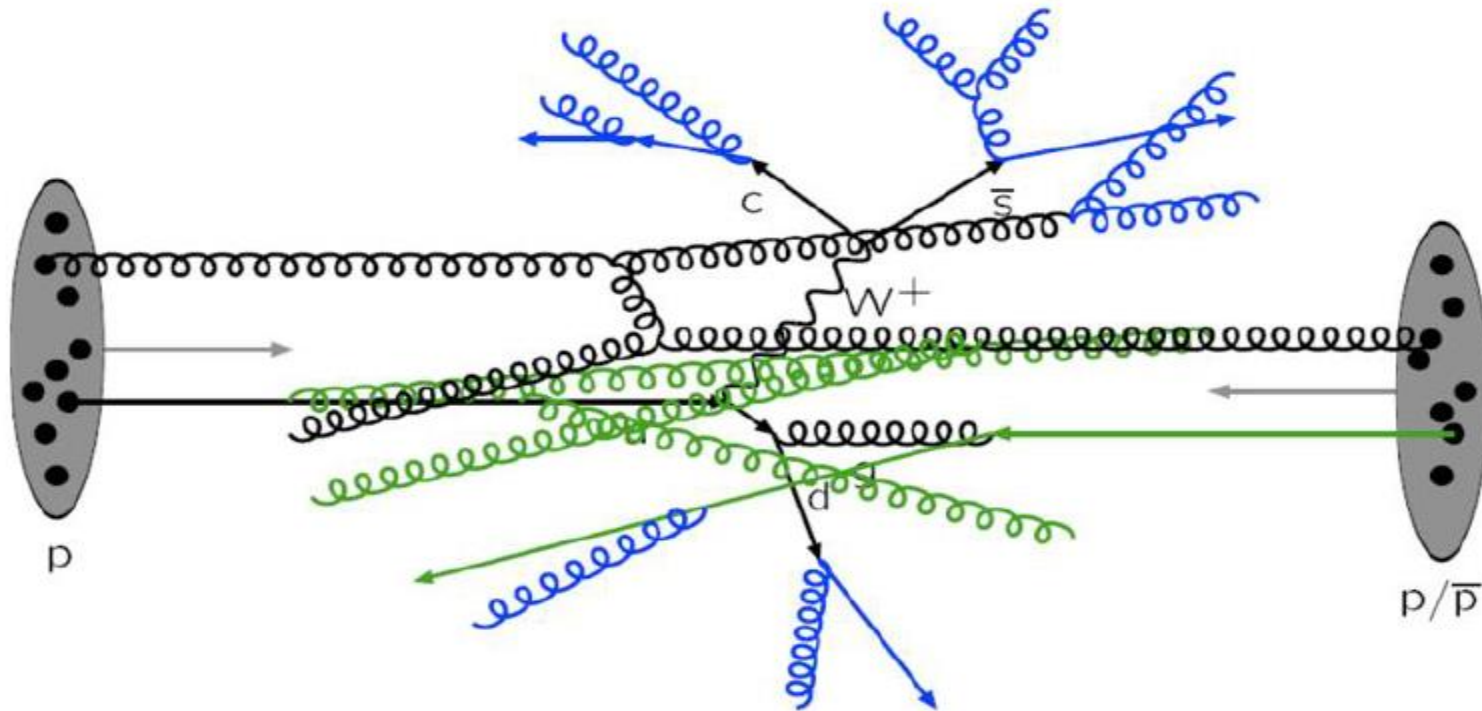
$[m_H \sim 120 \text{ GeV}]$

0.2% $H \rightarrow \gamma\gamma$

1.5% $H \rightarrow ZZ$

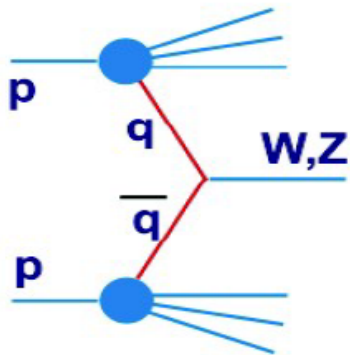
Proton-proton scattering at LHC

- Hard interaction: qq , gg , qg fusion
- Initial and final state radiation (ISR,FSR)
- Secondary interaction [“underlying event”]

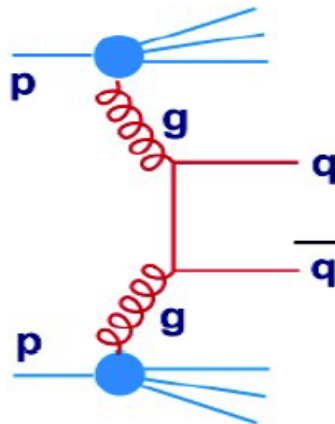


QCD hard scattering processes

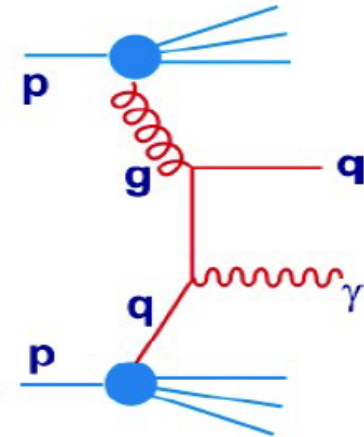
- EW gauge bosons



- Di-jets

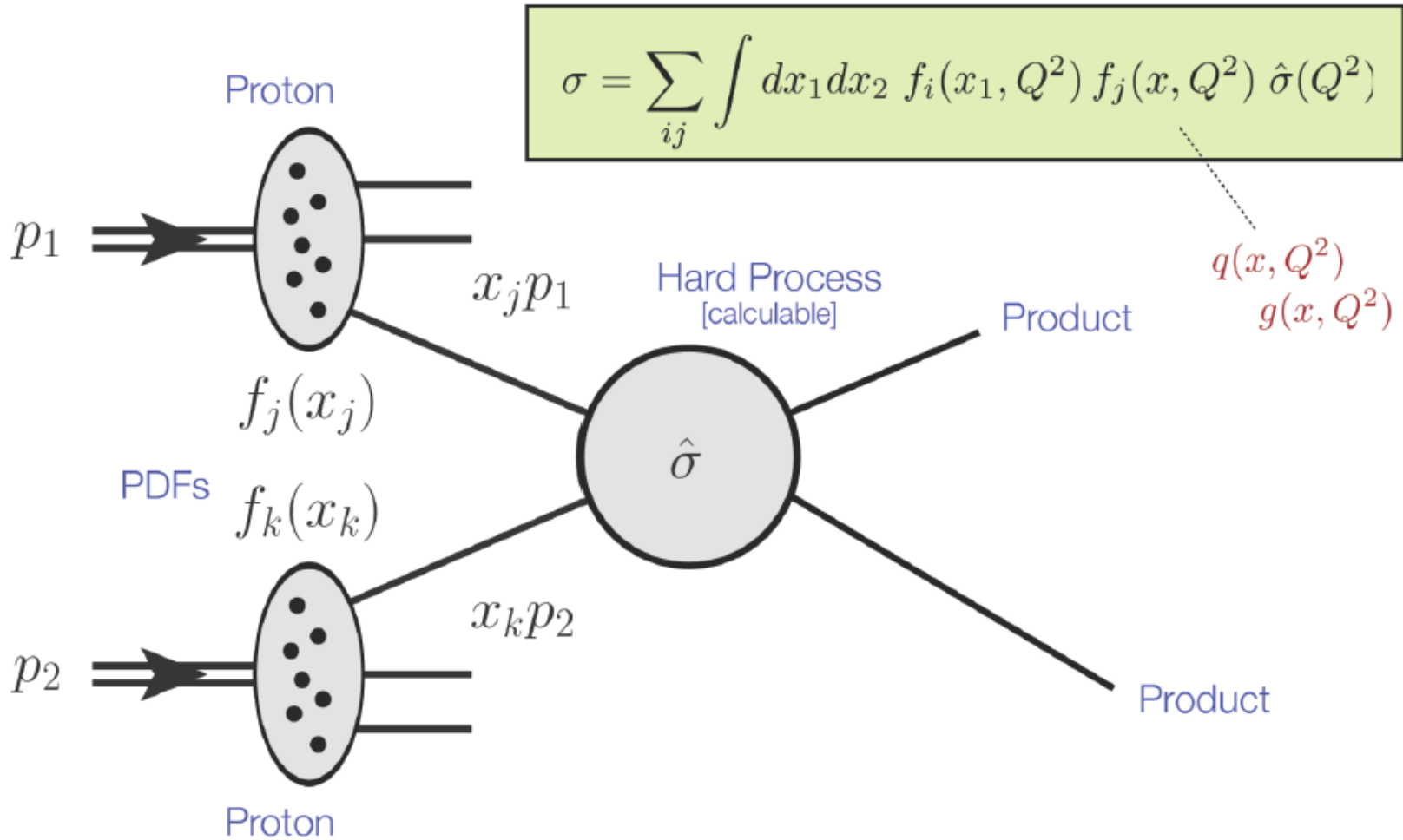


- Direct photons



- Measuring those processes test our understanding of:
 - Partonic structure of protons
 - QCD scattering via calculations of N(NLO)
 - Hadronisation/underlying event
 - What makes a good jet algorithm
 - Data driven background estimates for rare processes

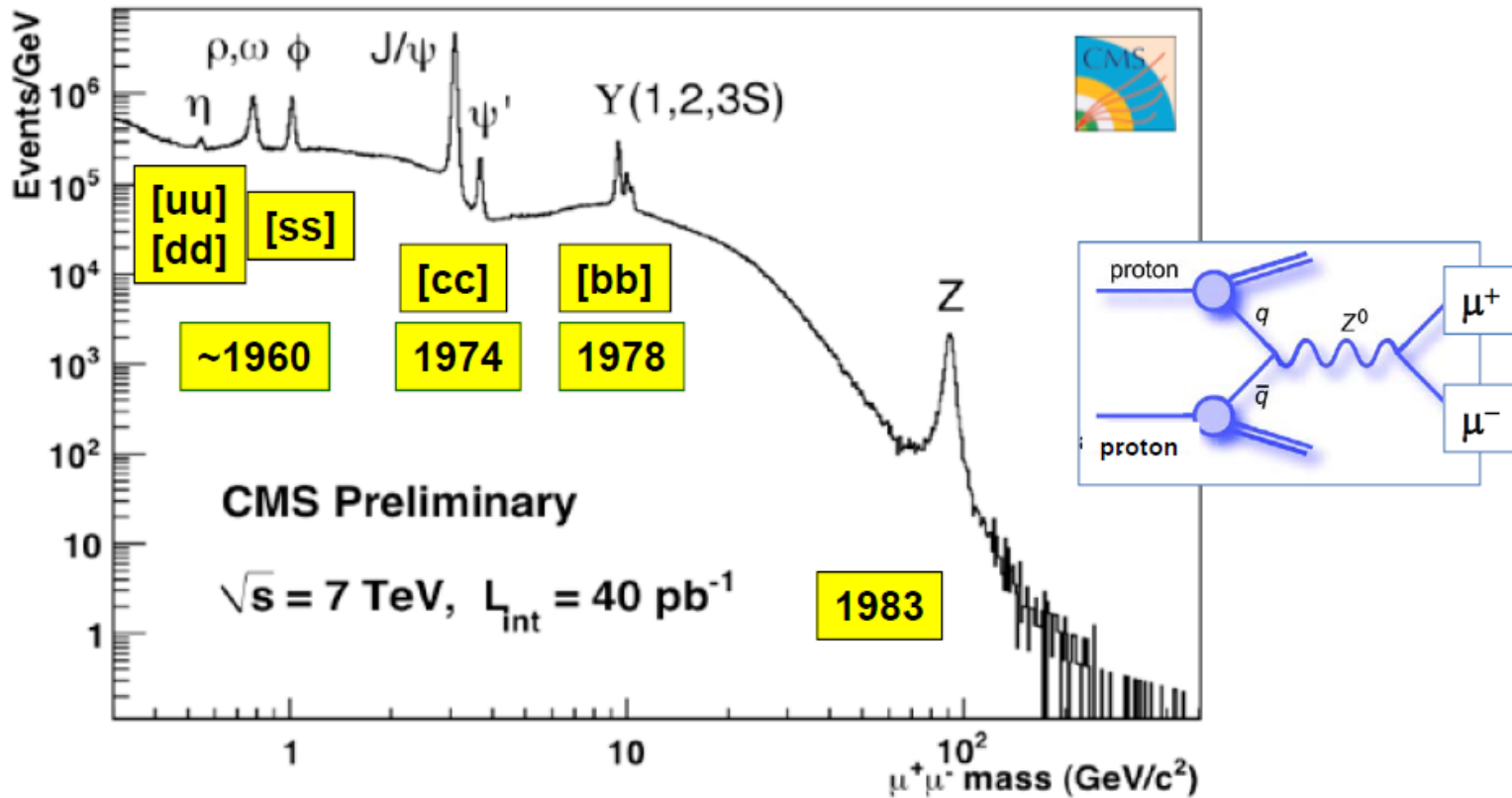
Proton-proton scattering at LHC



Year 2010: Retracing history of particle physics

2010

Data corresponding to $\sim 40 \text{ pb}^{-1}$ collected
→ re-discovery of the Standard Model



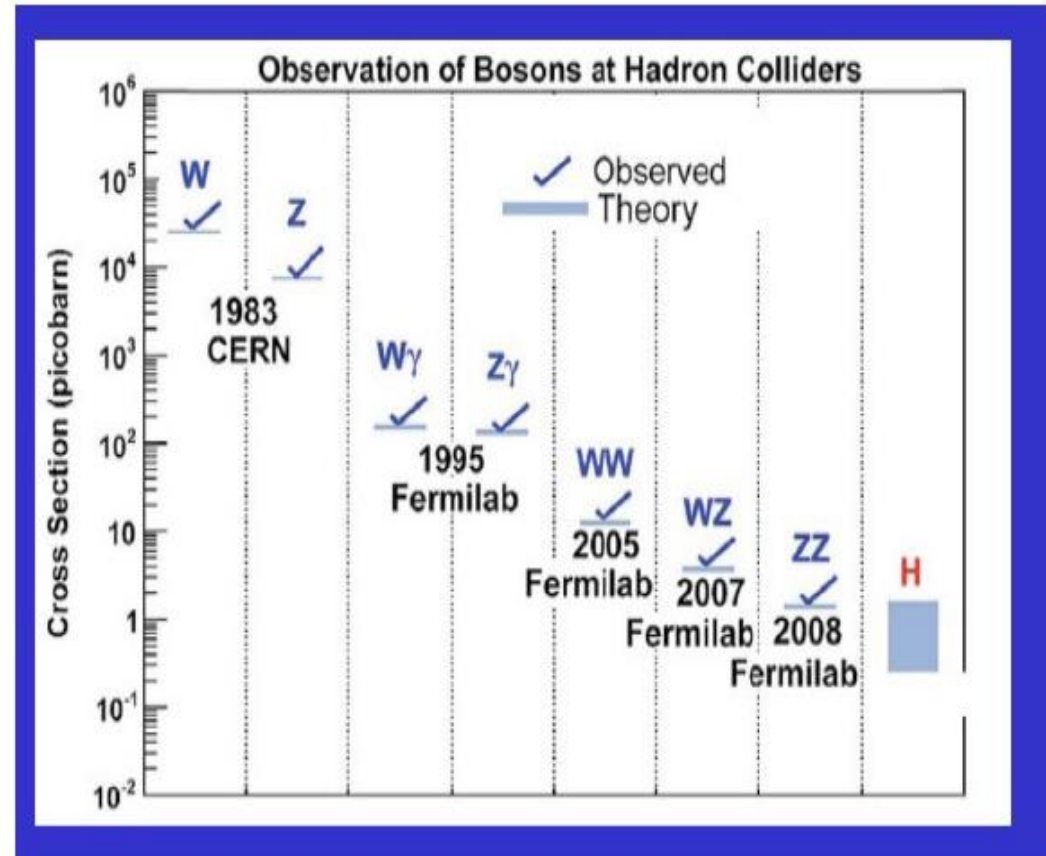
The di-muon spectrum recalls a long period of particle physics:
Well known quark-antiquark resonances (bound states) appear “online”

Bosons at hadron colliders

2010

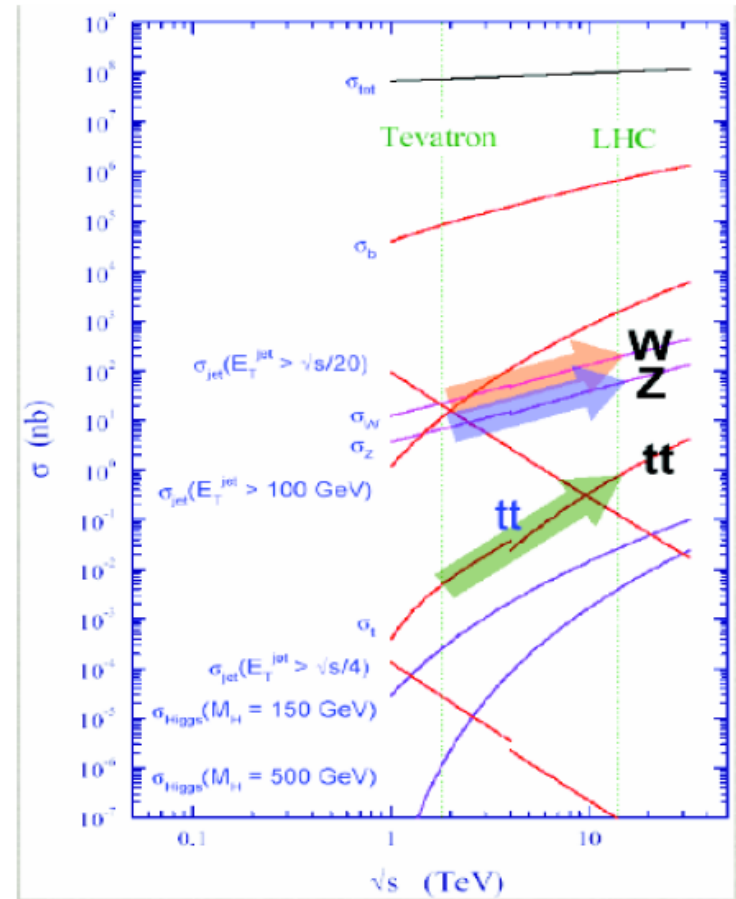
The primary decay channel is through leptonic decays:

- $BR(W \rightarrow e \nu) \sim 10\%$
- $BR(Z \rightarrow ee) \sim 3\%$
- It means that we are probing $\sigma \times BR$ values orders of magnitude smaller
- At LHC cross-section 5-10 x higher than at Tevatron at Fermilab.

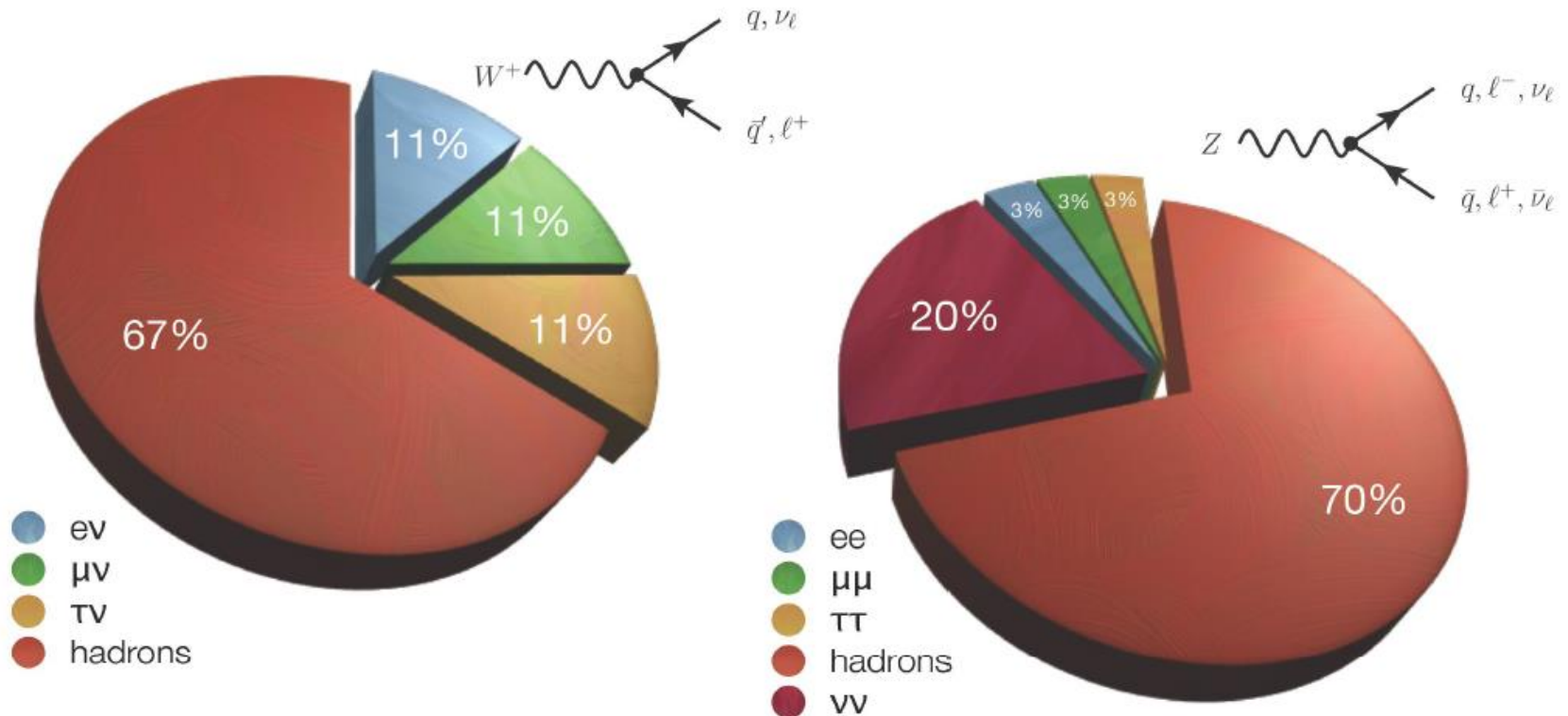


Bosons and top quark at LHC

- Well measured by previous experiments
- Still educational at LHC
 - Cross-sections
 - New PDF constraints
- „Standard candles” for high p_T analyses
 - Calibration, alignment
 - Independent luminosity measurements

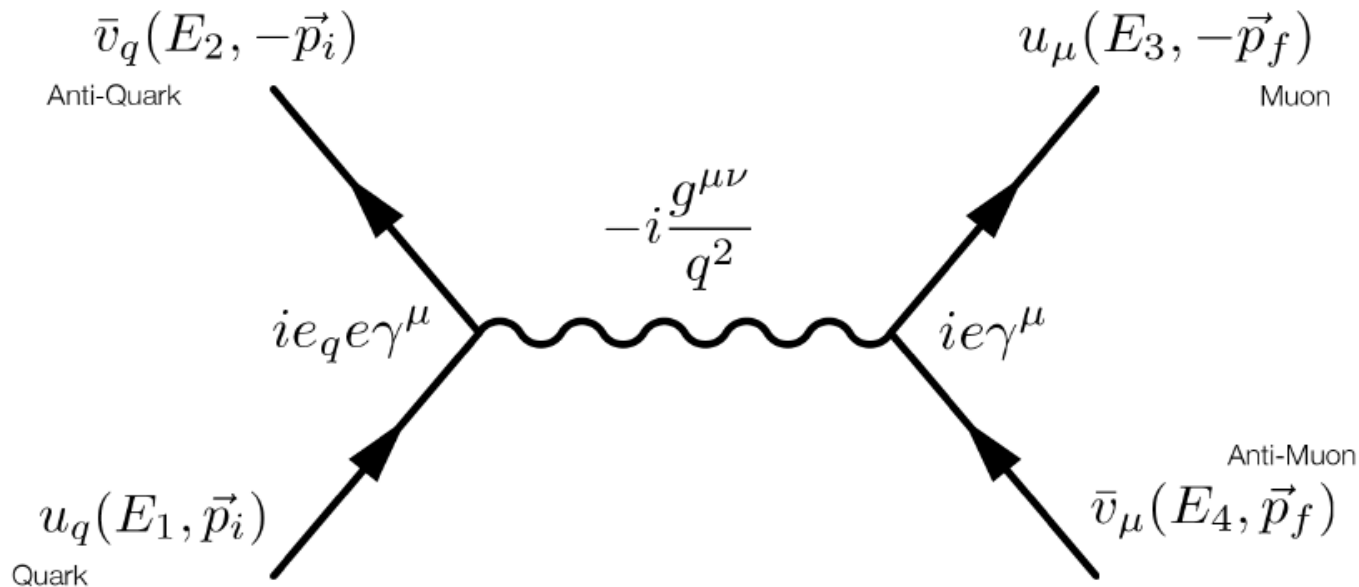


W and Z boson decays



Leptonic decays (e/ μ): very clean, but small(ish) branching fractions
 Hadronic decays: two-jet final states; large QCD dijet background
 Tau decays: somewhere in between...

Example: Drell-Yan process

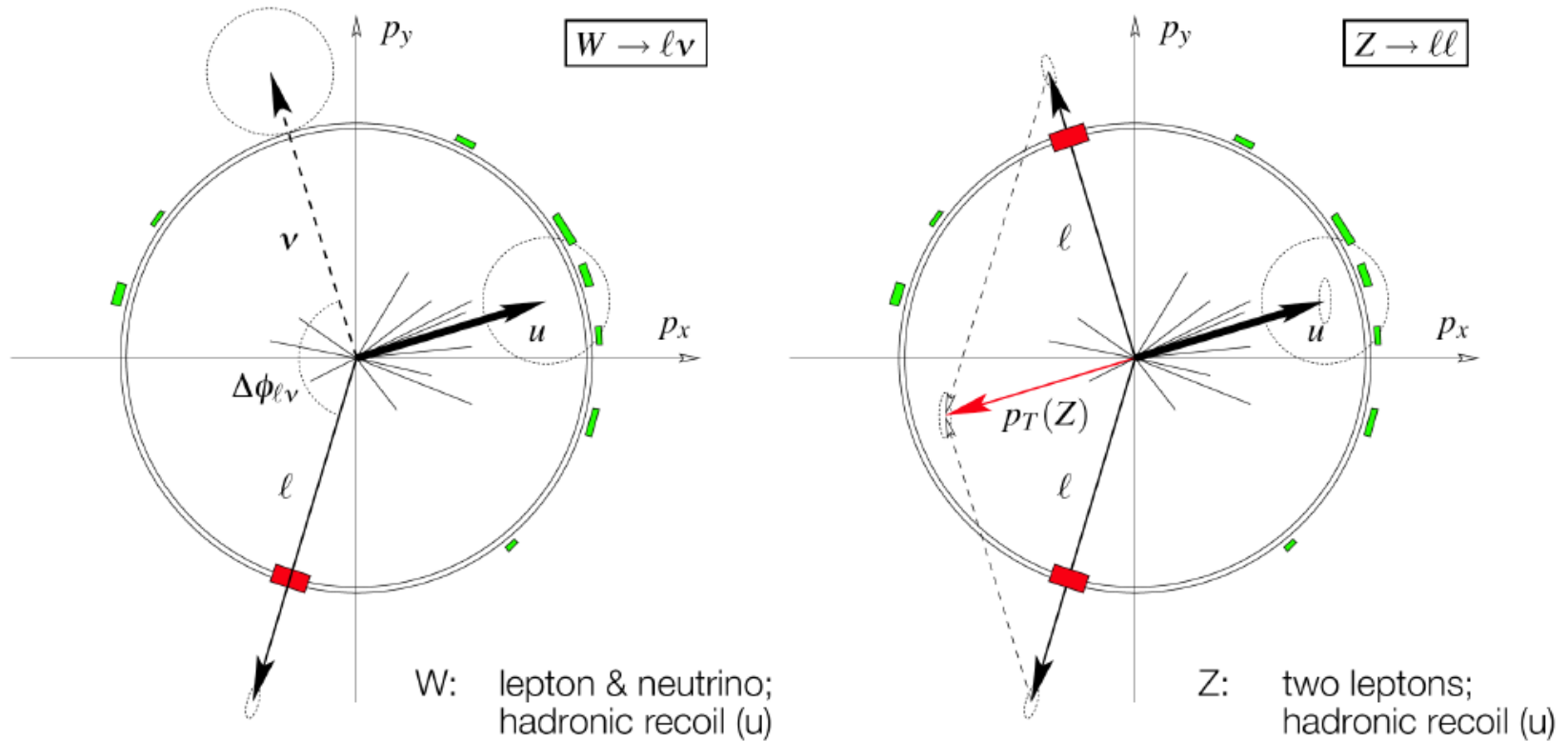


Averaging over initial spins

Summing over initial and final spins

$$|M_{fi}|^2 = \frac{1}{(2s_q + 1)^2} \cdot \sum_{s_q, s'_q} \sum_{s_\mu, s'_\mu} |M_{fi}|^2$$

W and Z boson signatures



Additional hadronic activity \rightarrow recoil, not as clean as e^+e^-
Precision measurements: only leptonic decays

Lepton identification

■ Electron:

- Compact electromagnetic cluster in calorimeter
- Matched to track

■ Muons:

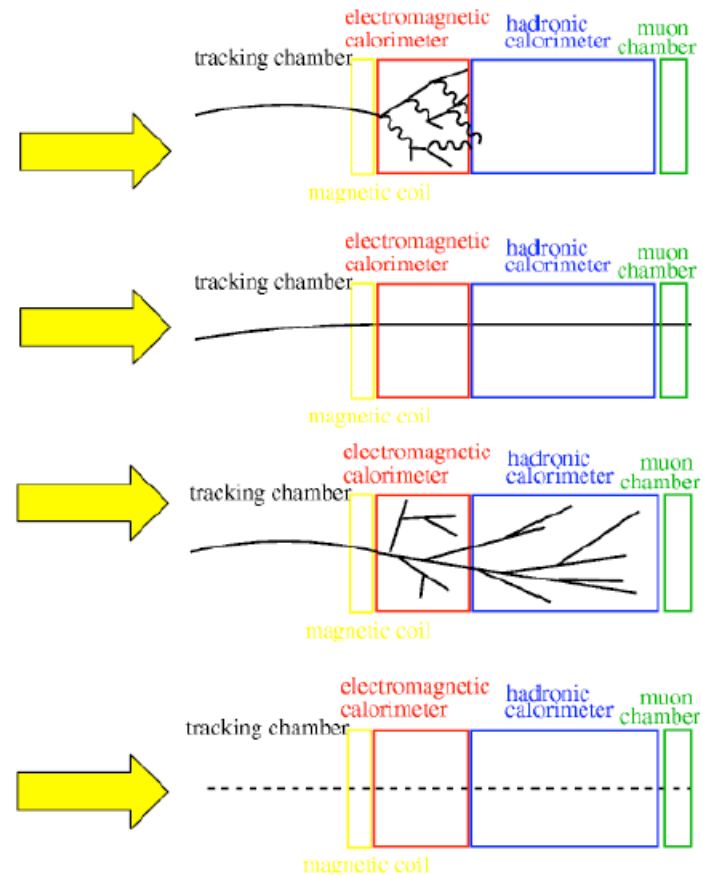
- Track in the muon chambers
- Matched to track

■ Taus:

- Narrow jet
- Matched to one or three tracks

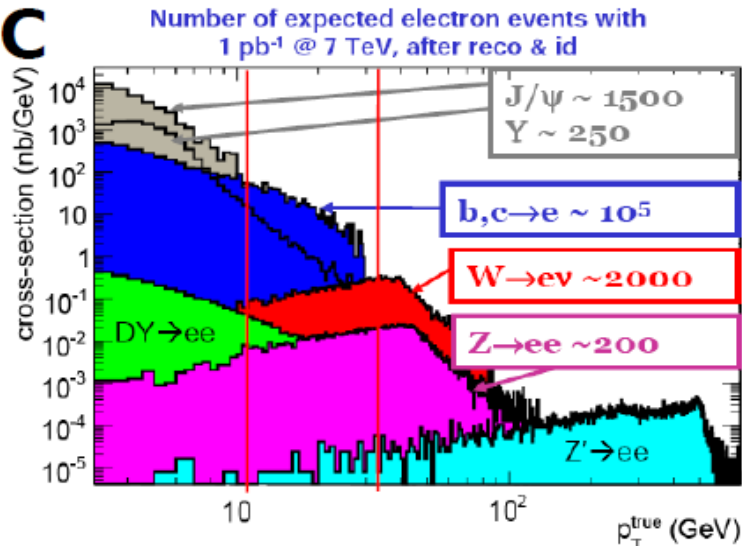
■ Neutrinos

- Imbalance in transverse momentum
- Inferred from total transverse energy in detector



Electrons and jets

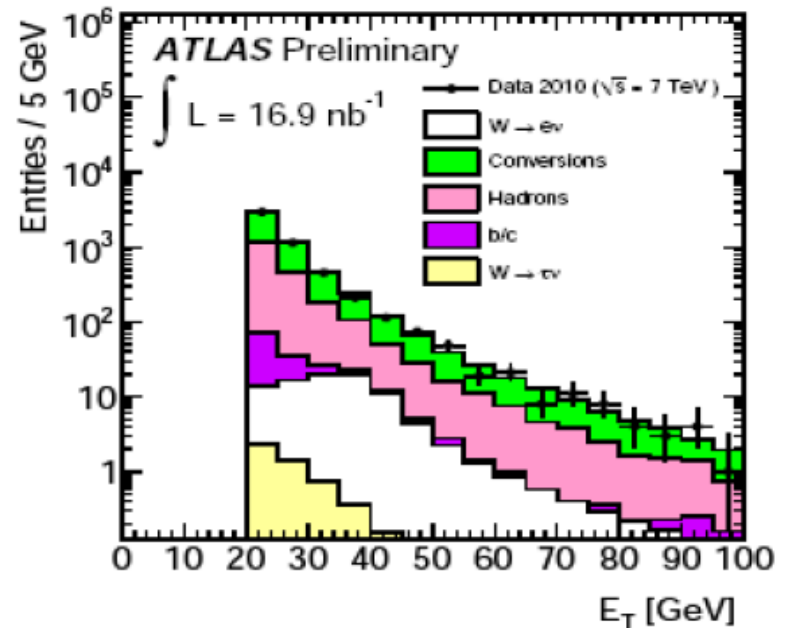
MC



- There is also lot of true electrons from semileptonic decays inside jets

- Jets can look like electrons
 - Photon conversion from π^0 's
 - Early showering charged pions
- And there is lot of jets
- Difficult to model in Monte Carlo
 - Detailed simulation in tracking and calorimeter volume

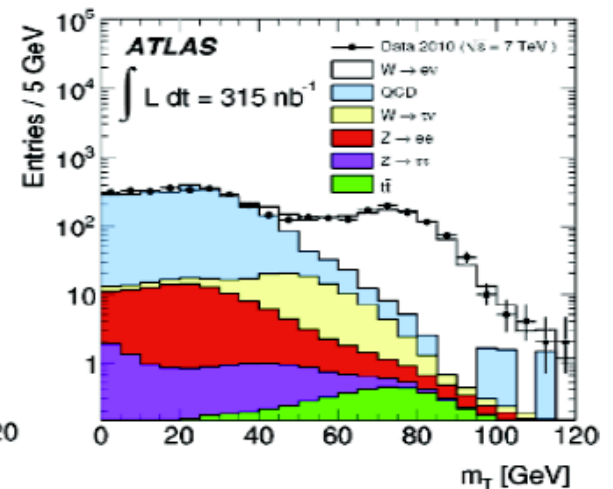
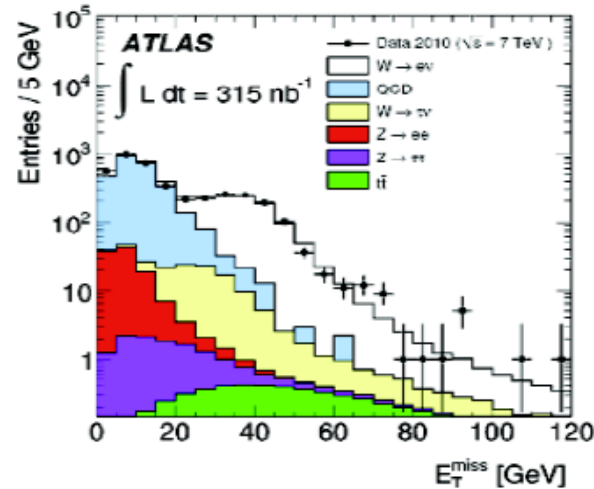
DATA: loose electron ID



W selection (2010)

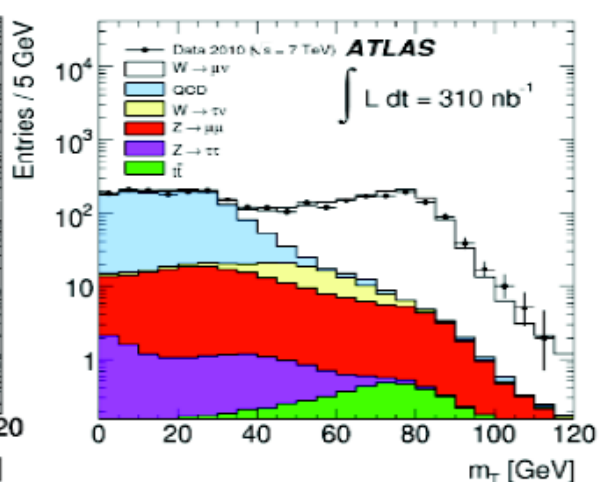
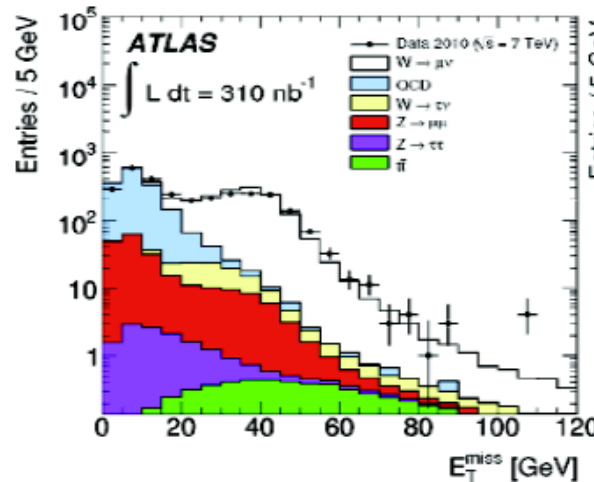
Electrons:

- $E_T > 20 \text{ GeV}$
- *Tight ID*
- *Missing $E_T > 25 \text{ GeV}$*
- $m_T > 40 \text{ GeV}$
- *1069 Candidates*



Muons:

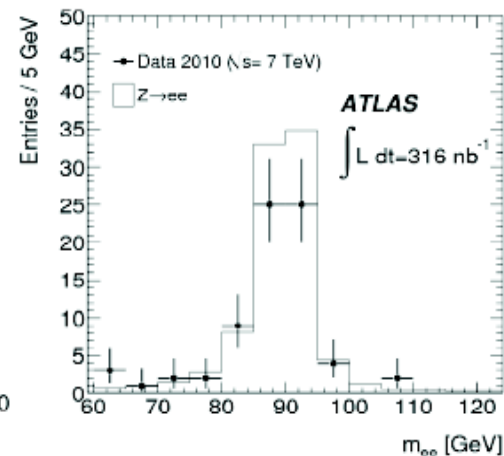
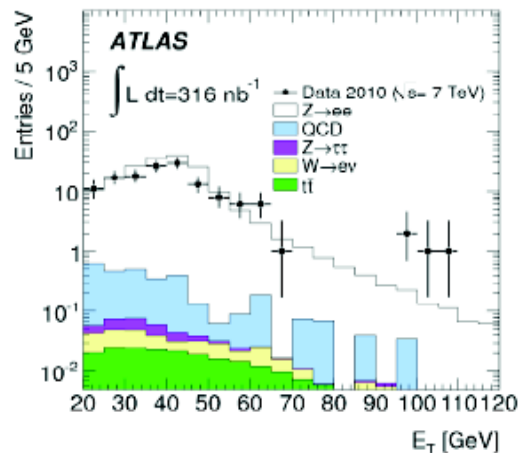
- $p_T > 20 \text{ GeV}$
- *Track isolation*
- *Missing $E_T > 25 \text{ GeV}$*
- $m_T > 40 \text{ GeV}$
- *1181 Candidates*



Z selection (2010)

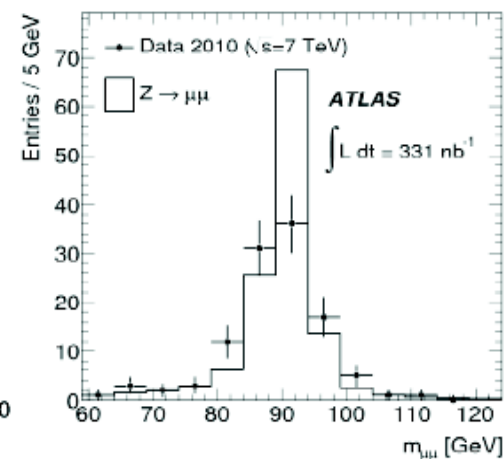
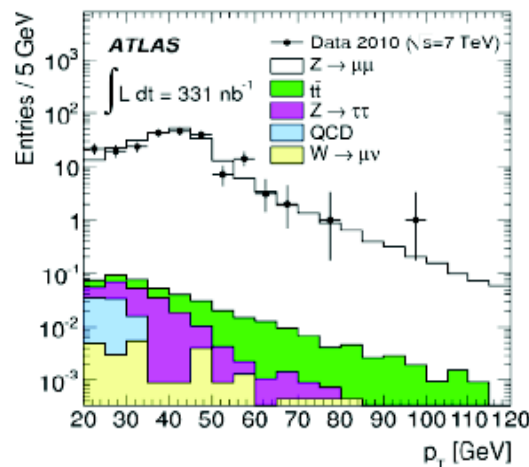
2 Electrons :

- $E_T > 20 \text{ GeV}$
- *Opposite charge*
- *Medium ID*
- $66 < m_{ee} < 116 \text{ GeV}$
- *70 Candidates*



2 Muons :

- $p_T > 20 \text{ GeV}$
- *Track isolation*
- *Opposite charge*
- $66 < m_{\mu\mu} < 116 \text{ GeV}$
- *109 Candidates*



W backgrounds

Electrons:

- EW + top background: $W \rightarrow \tau \nu + Z \rightarrow e^+e^- + t\bar{t}$

$$N_{EW+TOP} = 33.5 \pm 0.2(\text{stat}) \pm 3.0(\text{syst})$$

- QCD background is estimated with the template method using the missing energy distribution.

$$N_{QCD} = 28.0 \pm 3.0(\text{stat}) \pm 10.0(\text{syst})$$

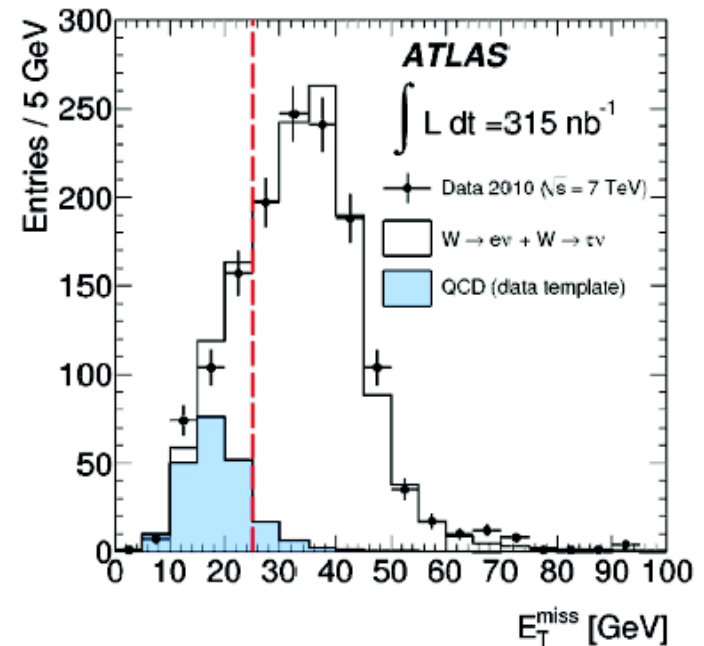
Muons:

- EW + top background: $Z \rightarrow \mu^+\mu^- + W \rightarrow \tau \nu + t\bar{t}$

$$N_{EW+TOP} = 77.6 \pm 0.3(\text{stat}) \pm 5.4(\text{syst})$$

- QCD background estimated from comparison of events seen in data after the full selection to number of events observed if the isolation is not applied.

$$N_{QCD} = 22.8 \pm 4.6(\text{stat}) \pm 8.7(\text{syst})$$



$$N_{loose} = N_{nonQCD} + N_{QCD}$$

$$N_{iso} = \epsilon_{nonQCD}^{iso} N_{nonQCD} + \epsilon_{QCD}^{iso} N_{QCD}$$

Cross-section & Luminosity

Number of observed events

just count ...

Background

measured from data or
calculated from theory

$$\sigma = \frac{N^{\text{obs}} - N^{\text{bkg}}}{\int \mathcal{L} dt \cdot \epsilon}$$

Luminosity

determined by accelerator,
triggers, ...

Efficiency

many factors, optimized
by experimentalist

W cross-section measurement

The total cross section for each lepton channel can be obtained by:

$$\sigma_W \times BR(W \rightarrow l\nu) = \frac{N_W^{obs} - N^{bkg}}{A_W C_W L_{int}}$$

A_W is the geometrical acceptance calculated at generator level:

$$A_W = \left(\frac{N^{acc}}{N^{all}} \right)_{gen}$$

MC	A_W $W^+ \rightarrow e^+\nu$	A_W $W^- \rightarrow e^-\nu$	A_W $W \rightarrow e\nu$	A_W $W^+ \rightarrow \mu^+\nu$	A_W $W^- \rightarrow \mu^-\nu$	A_W $W \rightarrow \mu\nu$
PYTHIA MRST LO*	0.466	0.457	0.462	0.484	0.475	0.480
PYTHIA CTEQ6.6	0.479	0.458	0.471	0.499	0.477	0.490
PYTHIA HERAPDF1.0	0.477	0.461	0.470	0.496	0.479	0.489
MC@NLO HERAPDF1.0	0.475	0.454	0.465	0.494	0.472	0.483
MC@NLO CTEQ6.6	0.478	0.452	0.465	0.496	0.470	0.483

W cross-section measurement

The total cross section for each lepton channel can be obtained by:

$$\sigma_W \times BR(W \rightarrow l\nu) = \frac{N_W^{obs} - N^{bkg}}{A_W C_W L_{int}}$$

A_W is the geometrical acceptance calculated at generator level:

$$A_W = \left(\frac{N^{acc}}{N^{all}} \right)_{gen}$$

MC	A_W $W^+ \rightarrow e^+\nu$	A_W $W^- \rightarrow e^-\nu$	A_W $W \rightarrow e\nu$	A_W $W^+ \rightarrow \mu^+\nu$	A_W $W^- \rightarrow \mu^-\nu$	A_W $W \rightarrow \mu\nu$
PYTHIA MRST LO*	0.466	0.457	0.462	0.484	0.475	0.480
PYTHIA CTEQ6.6	0.479	0.458	0.471	0.499	0.477	0.490
PYTHIA HERAPDF1.0	0.477	0.461	0.470	0.496	0.479	0.489
MC@NLO HERAPDF1.0	0.475	0.454	0.465	0.494	0.472	0.483
MC@NLO CTEQ6.6	0.478	0.452	0.465	0.496	0.470	0.483

C_W correction factor and uncertainties

$$\sigma_W \times BR(W \rightarrow l\nu) = \frac{N_W^{obs} - N^{bkg}}{A_W C_W L_{int}}$$

- C_W is a factor correcting for reconstruction, identification and trigger efficiencies of the lepton.

	$W \rightarrow e\nu$	$W \rightarrow \mu\nu$
C_W	0.66	0.76

- Components to systematic uncertainties, are summarized below:

Parameter	$\delta C_W / C_W (\%)$
Trigger efficiency	<0.2
Material effects, reconstruction and identification	5.6
Energy scale and resolution	3.3
E_T^{miss} scale and resolution	2.0
Problematic regions in the calorimeter	1.4
Pile-up	0.5
Charge misidentification	0.5
FSR modelling	0.3
Theoretical uncertainty (PDFs)	0.3
Total uncertainty	7.0

Electrons

Parameter	$\delta C_W / C_W (\%)$
Trigger efficiency	1.9
Reconstruction efficiency	2.5
Momentum scale	1.2
Momentum resolution	0.2
E_T^{miss} scale and resolution	2.0
Isolation efficiency	1.0
Theoretical uncertainty (PDFs)	0.3
Total uncertainty	4.0

Muons

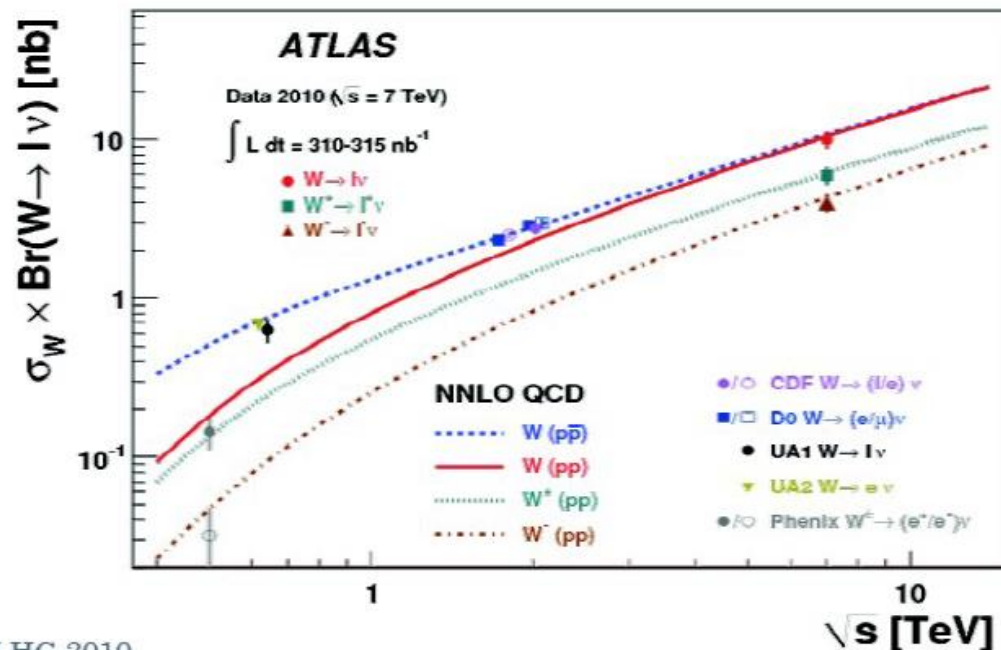
W cross-section measurement

$$L \approx 310 - 315 \text{ nb}^{-1}$$

Theory prediction : $10.46 \pm 0.42 \text{ nb}$

$$\sigma_W \times BR(W \rightarrow e\nu) = [10.51 \pm 0.34(\text{stat}) \pm 0.81(\text{sys}) \pm 1.16(\text{lumi})] \text{ nb}$$

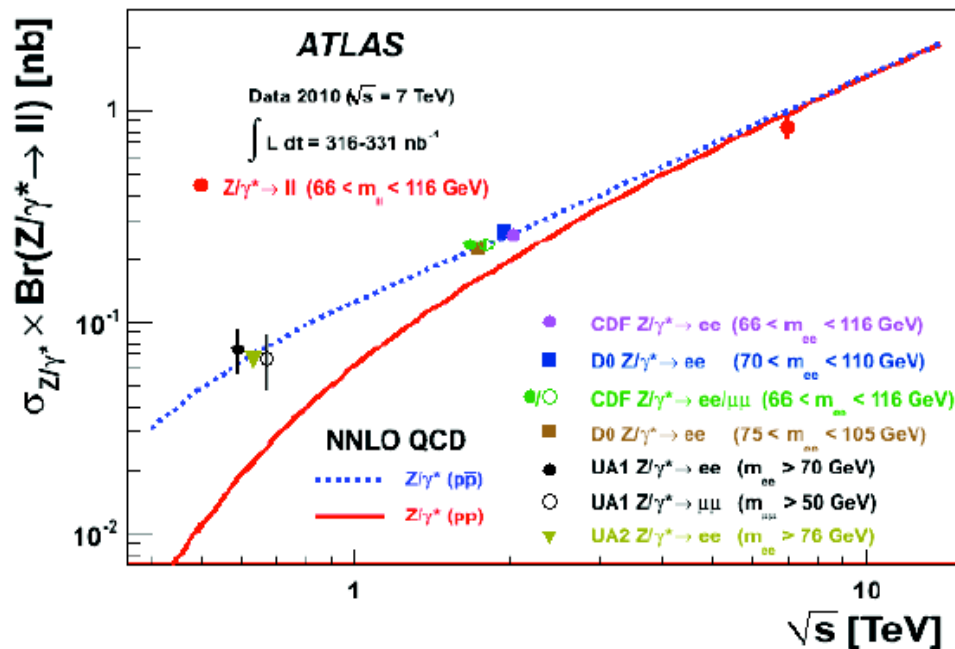
$$\sigma_W \times BR(W \rightarrow \mu\nu) = [9.58 \pm 0.30(\text{stat}) \pm 0.50(\text{sys}) \pm 1.05(\text{lumi})] \text{ nb}$$



Z cross-section measurement

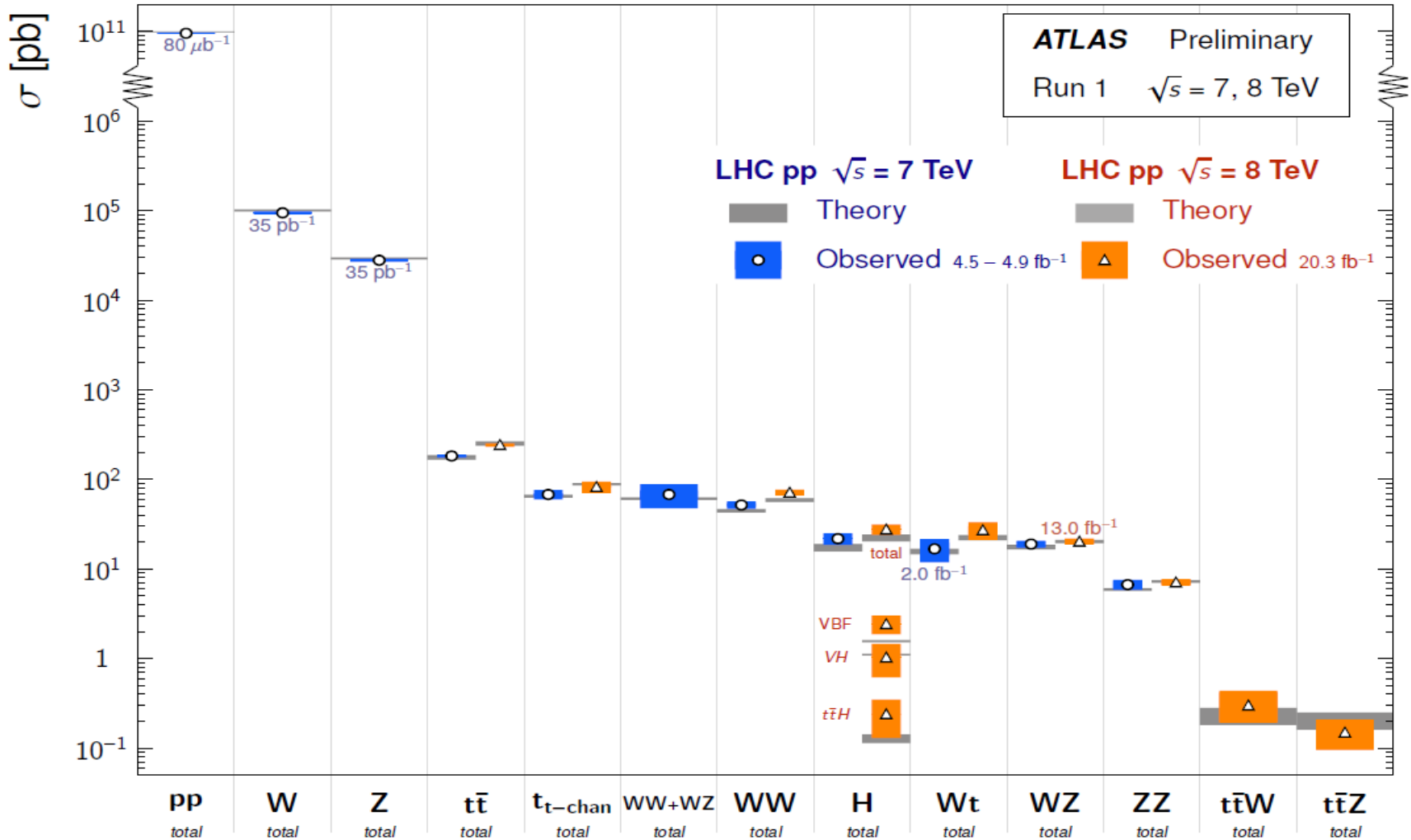
$L \approx 310 - 315 \text{ nb}^{-1}$

Theory prediction : $0.96 \pm 0.04 \text{ nb}$ for $[66 - 116] \text{ GeV}$ mass window
 $\sigma_Z \times BR(Z \rightarrow e^+e^-) = [0.75 \pm 0.09(\text{stat}) \pm 0.08(\text{sys}) \pm 0.08(\text{lumi})] \text{ nb}$
 $\sigma_Z \times BR(Z \rightarrow \mu^+\mu^-) = [0.87 \pm 0.08(\text{stat}) \pm 0.06(\text{sys}) \pm 0.10(\text{lumi})] \text{ nb}$

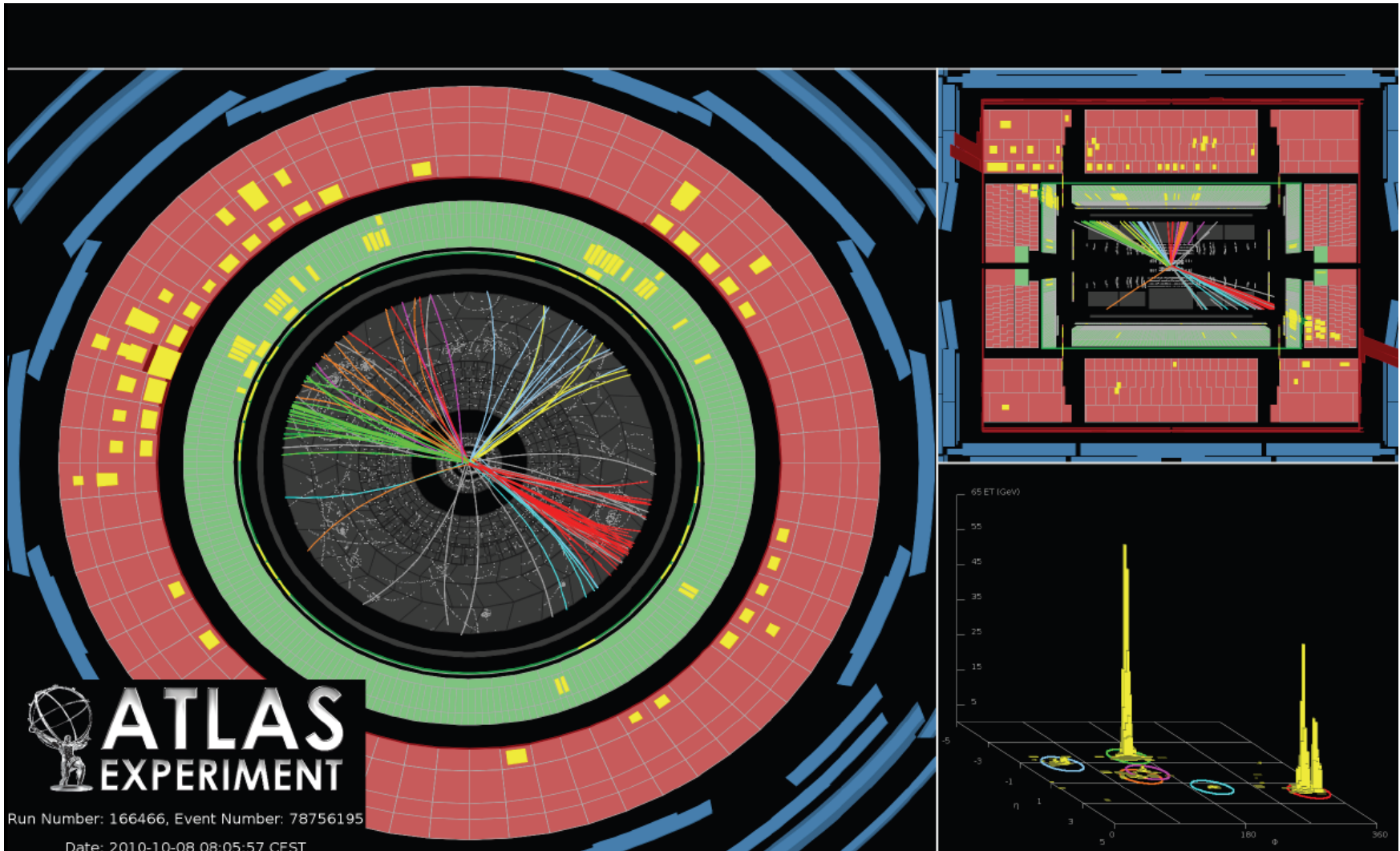


Production cross-sections

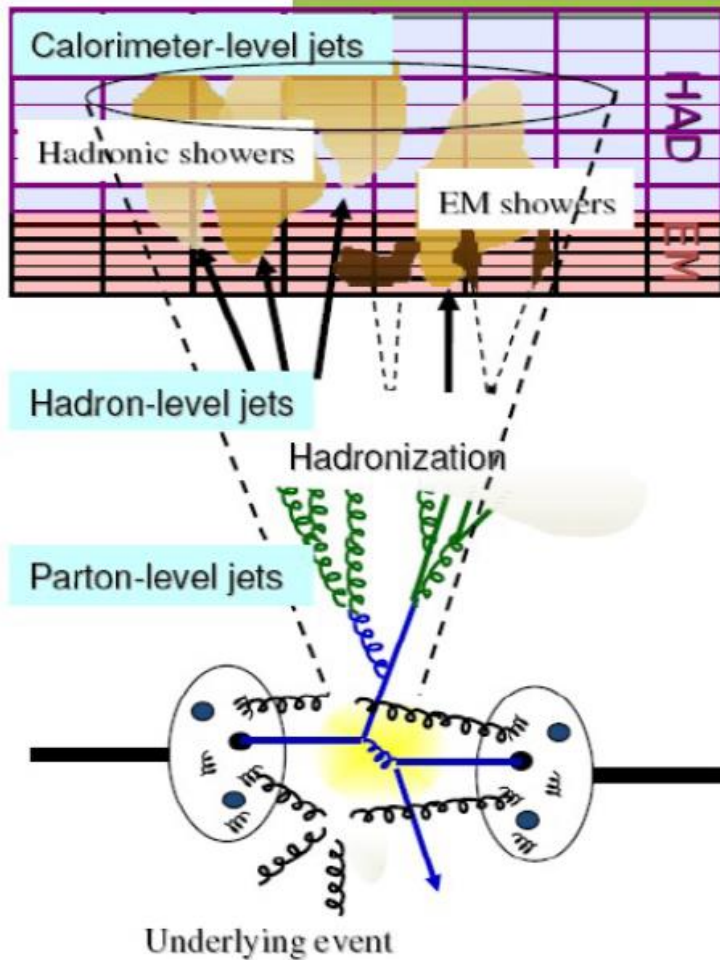
Standard Model Total Production Cross Section Measurements Status: March 2015



Confinement, hadronisation, jets....



Inclusive jet production



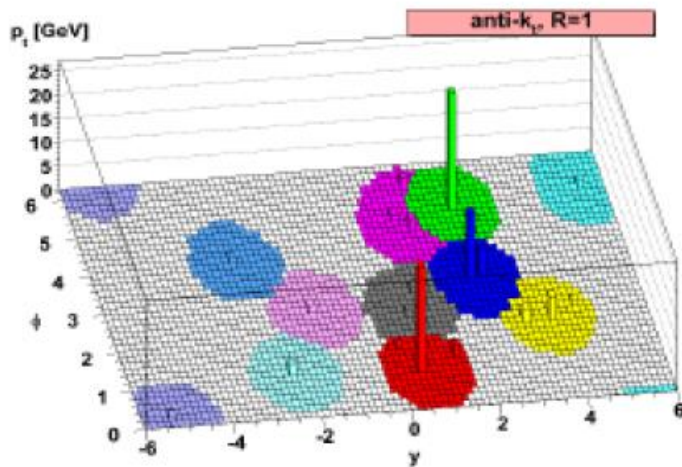
Unfold measurements to the hadron (particle) level

Correct parton-level theory for non-perturbative effects (hadronization & underlying event)

Jets are collimated spray of particles originating from parton fragmentation.
→ To be defined by an algorithm

Jet reconstruction

- Jet finding: from partons/particles/energy deposits to jet

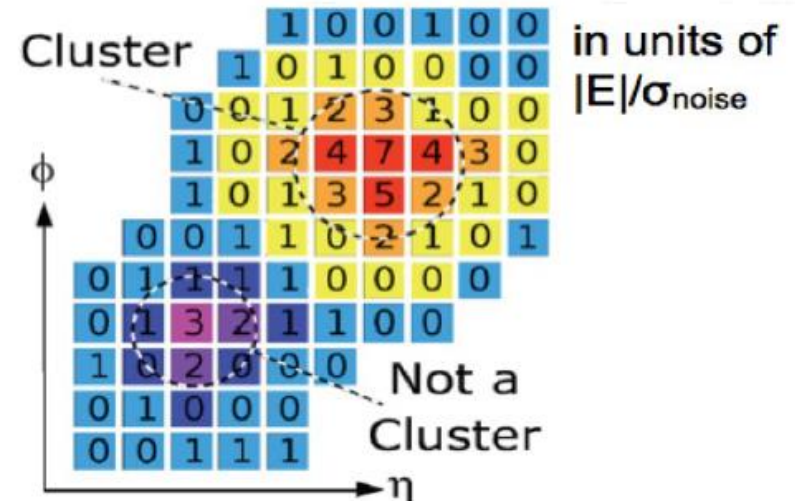


[Cacciari, Salam, Soyez
JHEP 0804:063,2008]

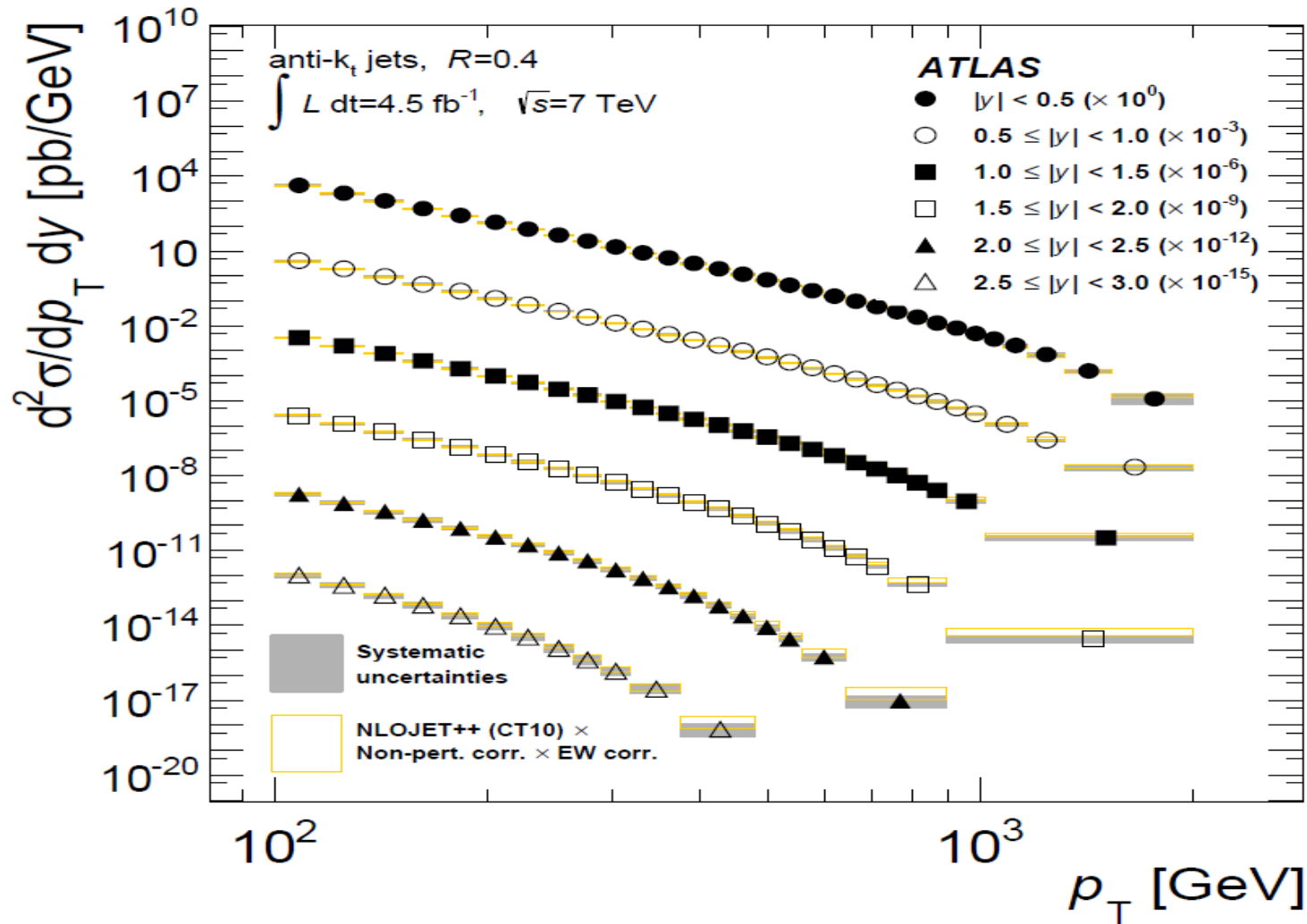
Energy deposits \rightarrow noise-suppressed **3D clusters**:
exploit transverse and longitudinal calorimeter segmentation

Jet inputs clustered with **anti- k_T** algorithm:

- Infrared safe, collinear safe (\Rightarrow NLO comparisons)
- Regular, cone-like jets in calorimeters
- Distance parameter 0.4, 0.6

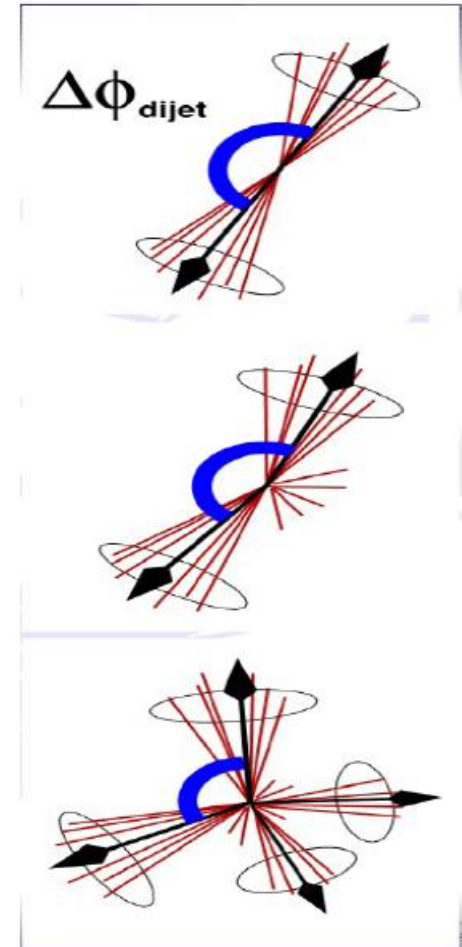


Di-jet cross-section



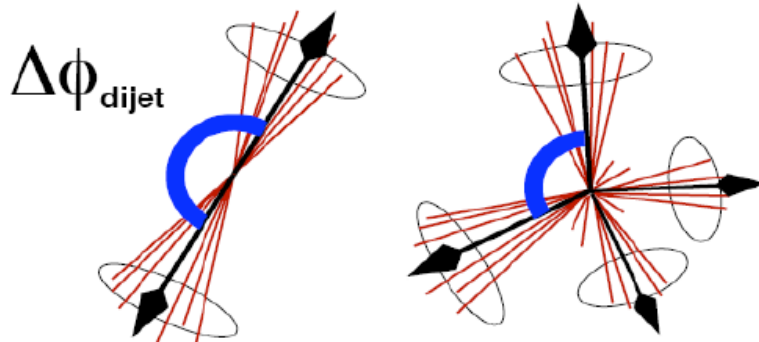
Multi-jet events

- Azimuthal decorrelations in dijet events and distribution of energy within jets sensitive to QCD radiation structures
 - Probing higher order QCD radiation
 - Main systematics: cluster energy scale (separate from JES) and unfolding

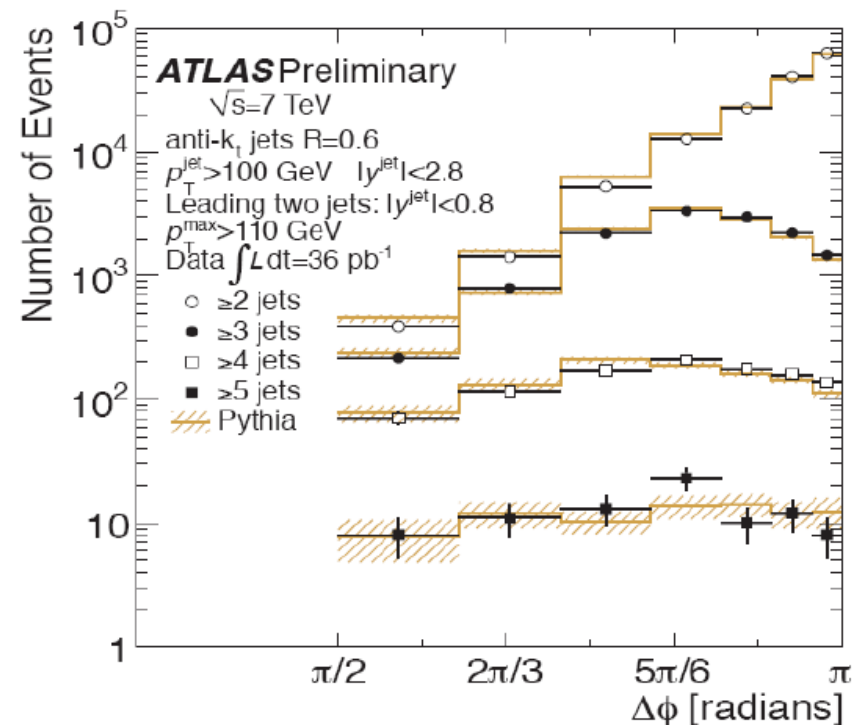


Azimuthal decorrelations

- Complementary to multi-jet cross section measurement.
- Pure di-jets have azimuthal angle Φ between jets equal to π .
- With additional hard radiation, i.e. extra jets, phi becomes smaller.



- Requiring additional jets flattens distribution.

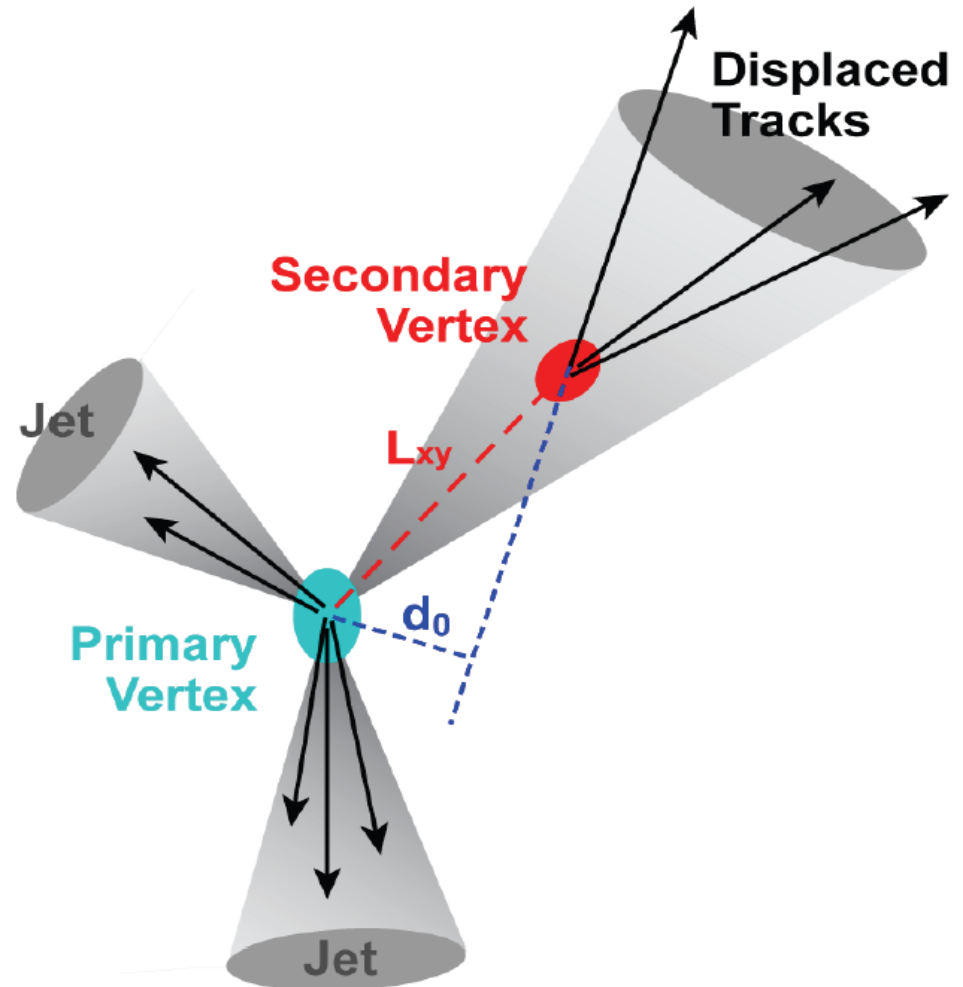


Confinement, hadronisation, jets....

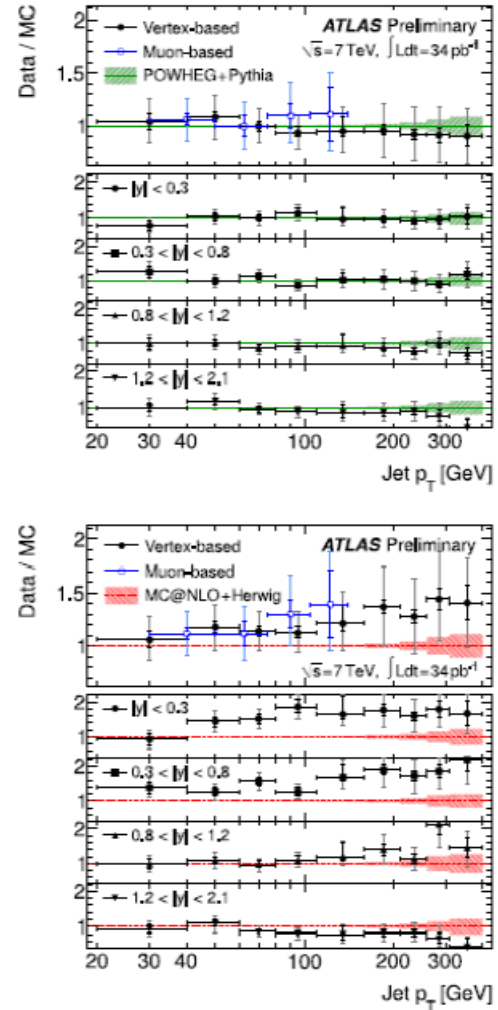
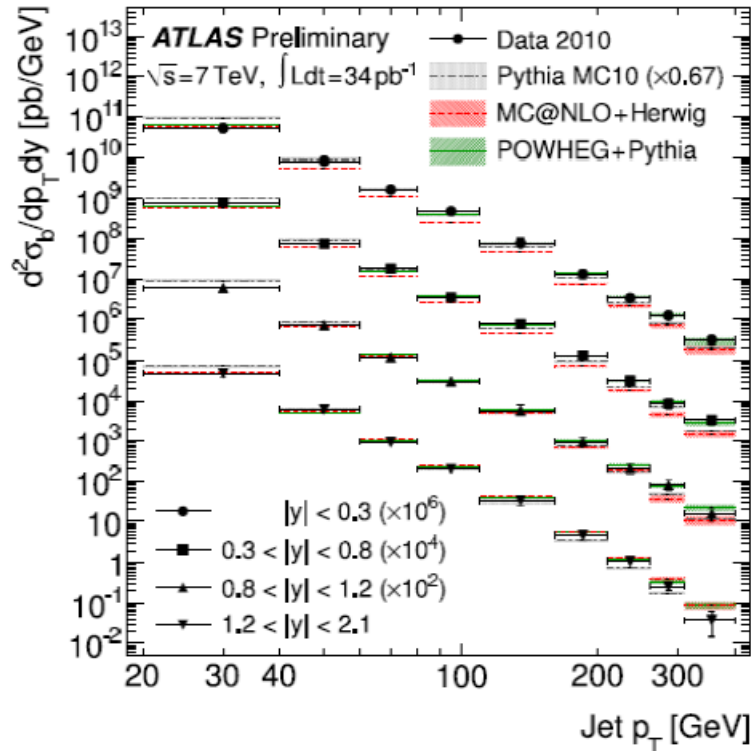
B-tagging



- When a b quark is produced, the associated jet will very likely contain at least one B meson or hadron
- B mesons/hadrons have relatively long lifetime
 - ✓ They will travel away from collision point before decaying
- Identifying a secondary decay vertex in a jet allow to tag its quark content
- Similar procedure for c quark...

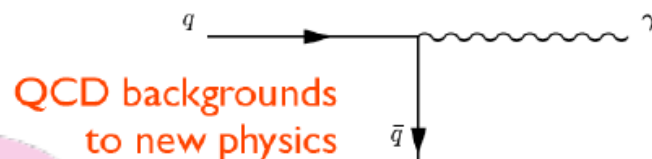
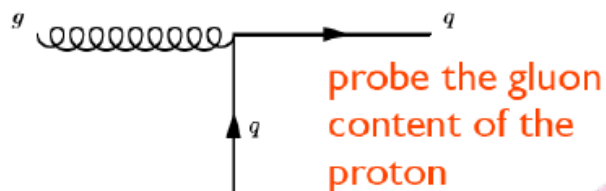


b-jet cross-sections

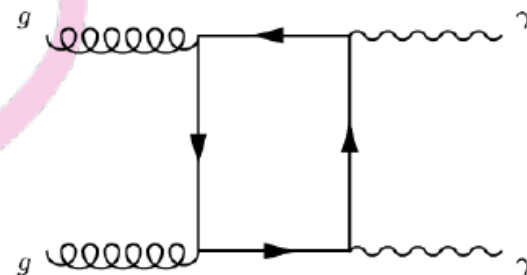
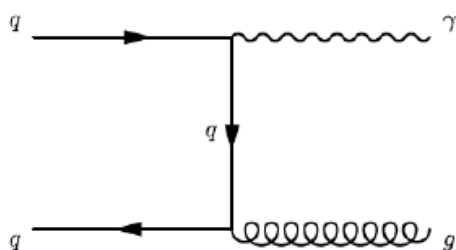


- Good agreement with Powheg+PYTHIA
- MC@NLO+Herwig predicts too few central jets, too many forward jets

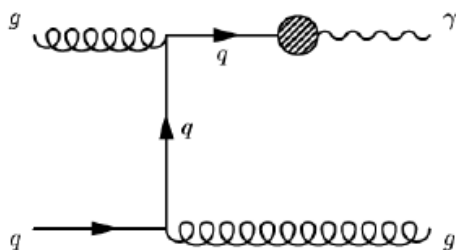
Why measure prompt photons



test
NLO pQCD
 predictions using
 a measurement
 without jets

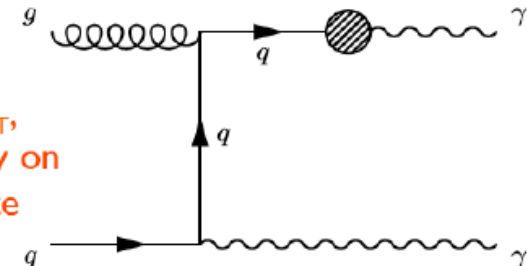


resummation



k_T factorisation

fragmentation important at low E_T ,
 suppressed by isolation cut. MCs rely on
 fragmentation function to compute



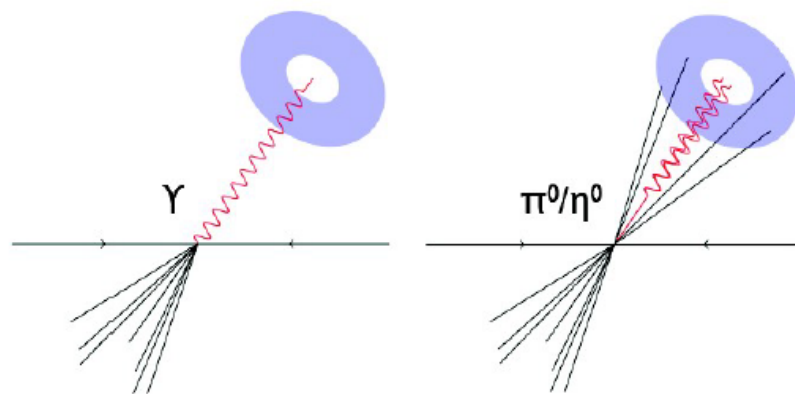
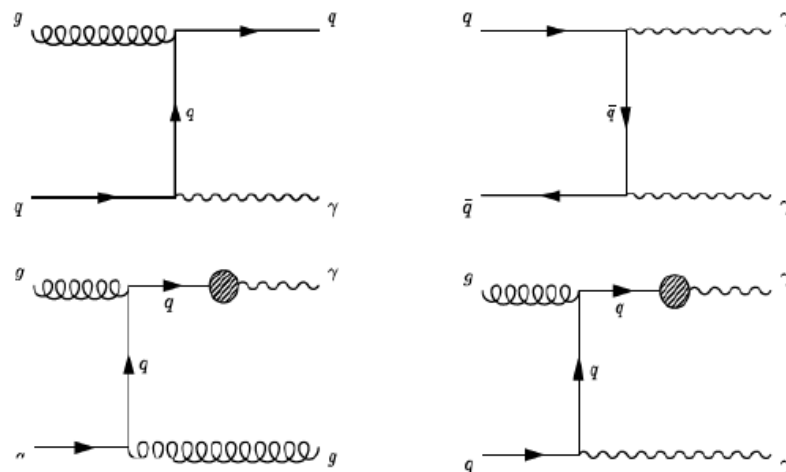
Prompt and isolated photons

■ Prompt:

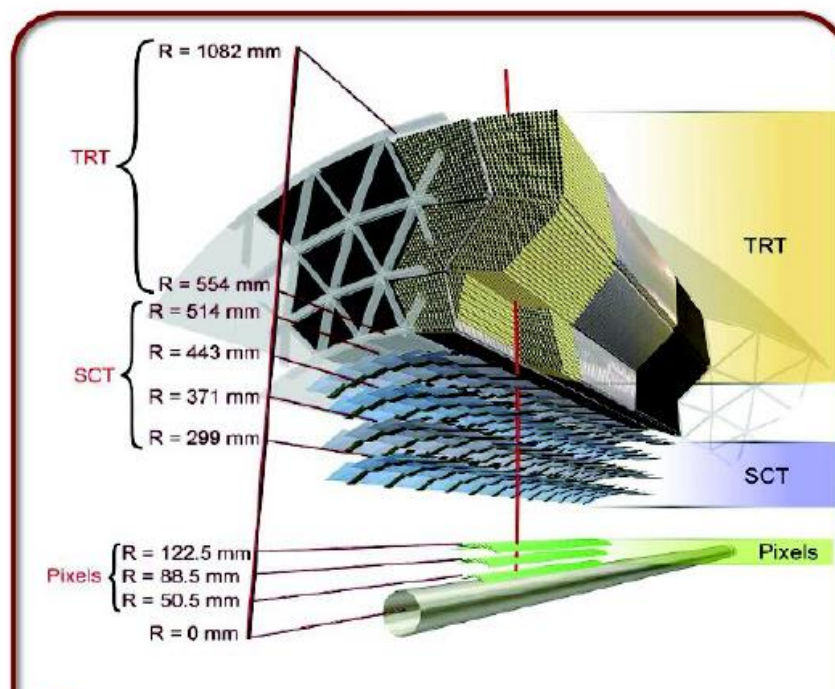
- Direct from the hard scattering
- Parton fragmentation more important at low E_T

■ Isolated:

- Isolation criteria to reduce bgd from QCD jets
 - Photons from neutral meson decay in jets
- Reduced fragmentation component:
 - $\sim 30\%$ reduction at 15 GeV
 - $< 10\%$ above 35 GeV

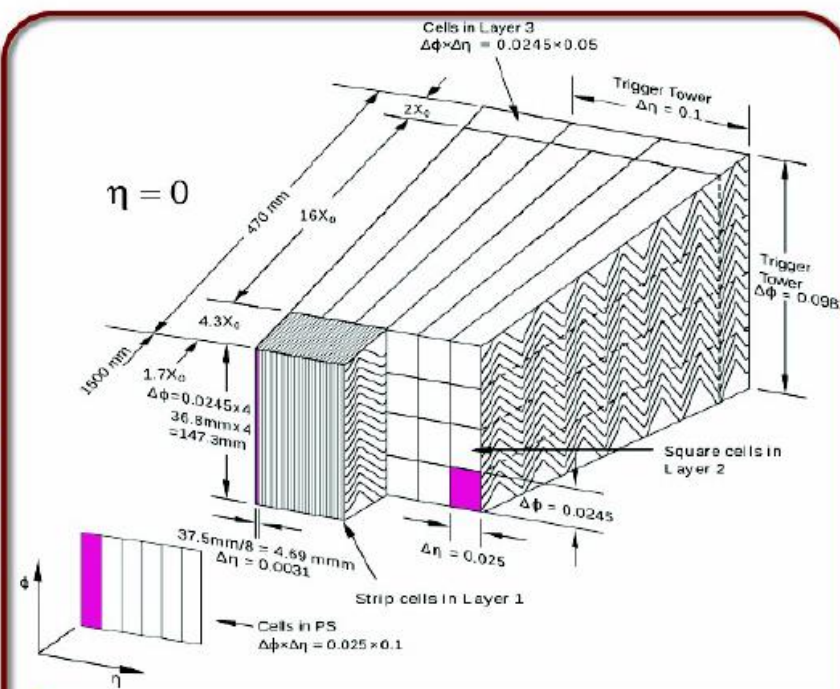


Measuring photons with ATLAS



- **Inner detector**

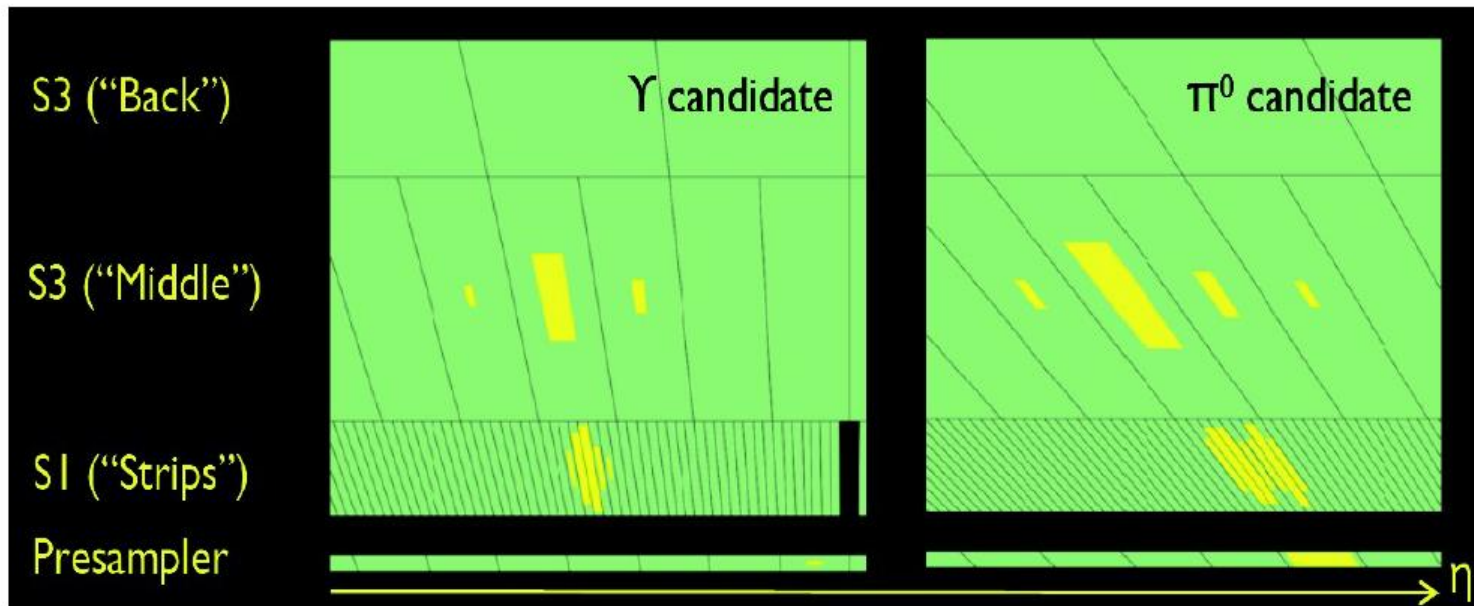
- ✓ track charged particles
- ✓ measure transition radiation
- ✓ **e/γ discrimination**
- ✓ **γ conversion reconstruction**



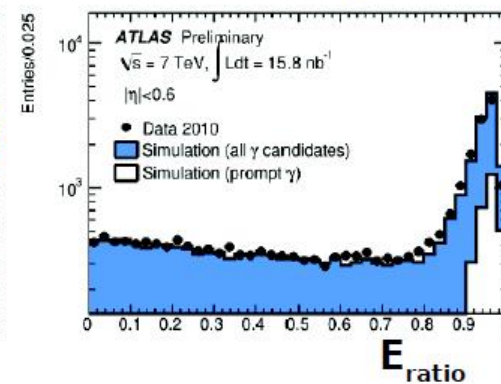
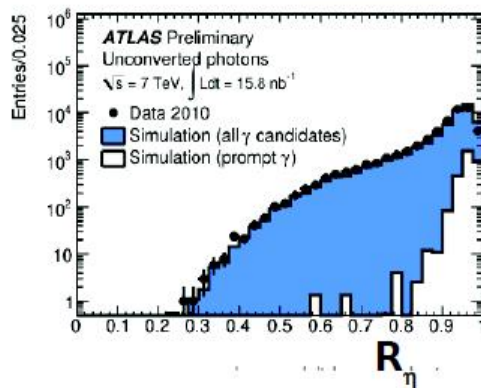
- **Pb-LAr EM calorimeter**

- ✓ η/ϕ /longitudinal segmentation
- ✓ fine granularity in 1st layer up to $\eta < 2.37$
- ✓ **γ energy and direction**
- ✓ **γ/π⁰ separation (EM shower moments)**

Photon identification

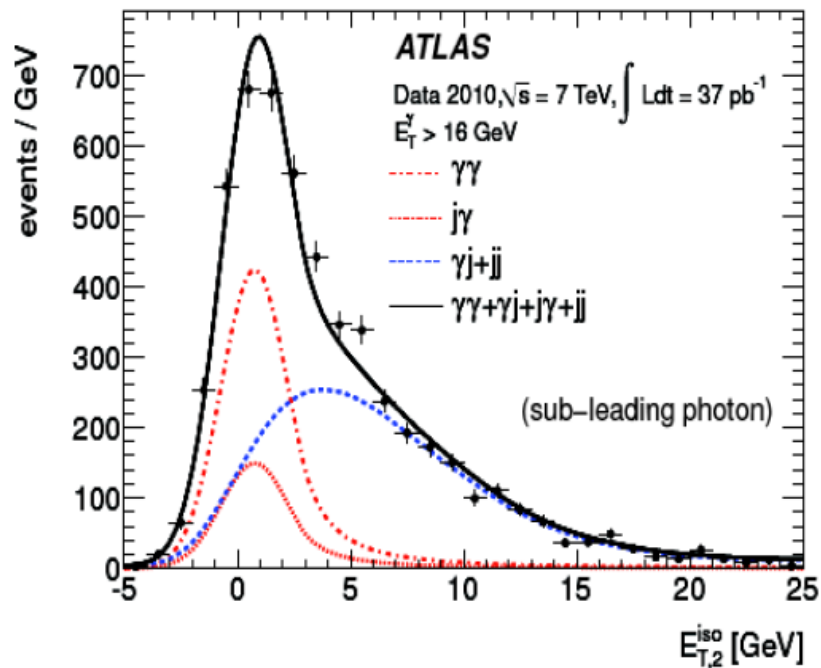
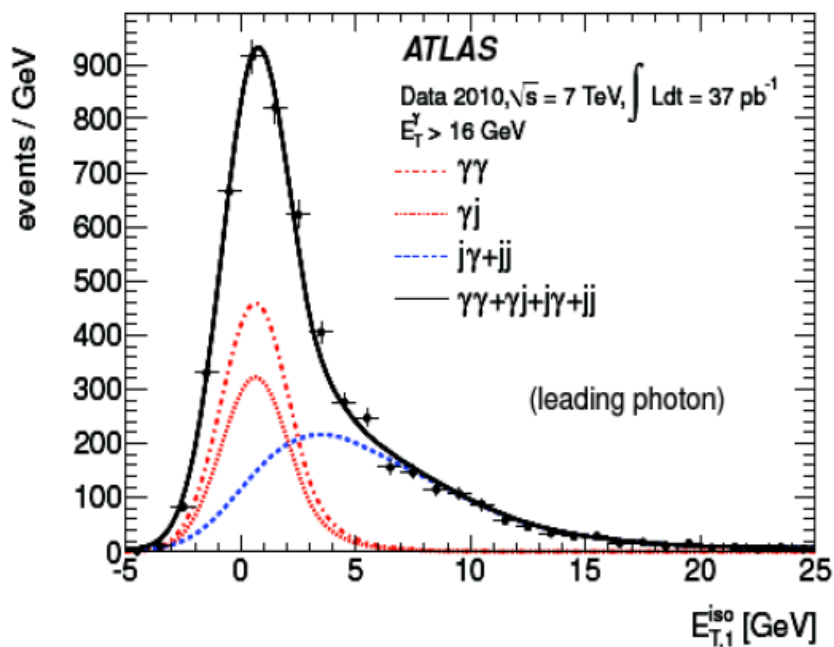


- loose and tight selection
- optimised separately for unconverted and converted photons

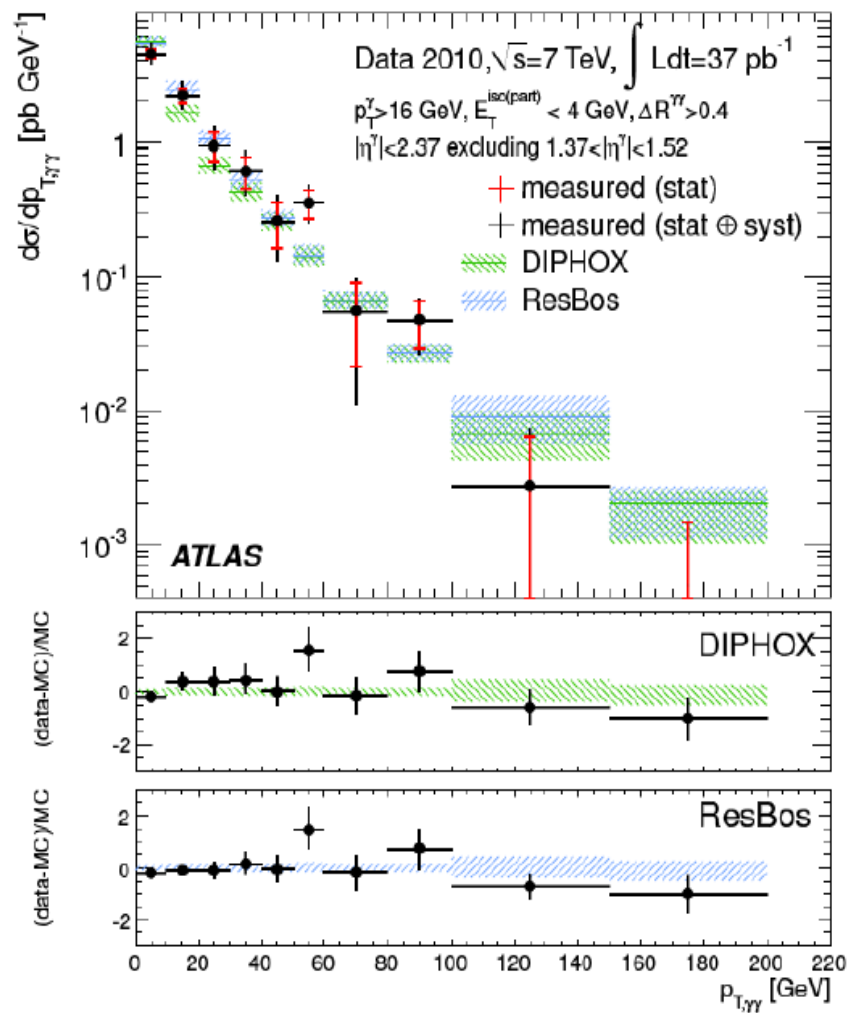
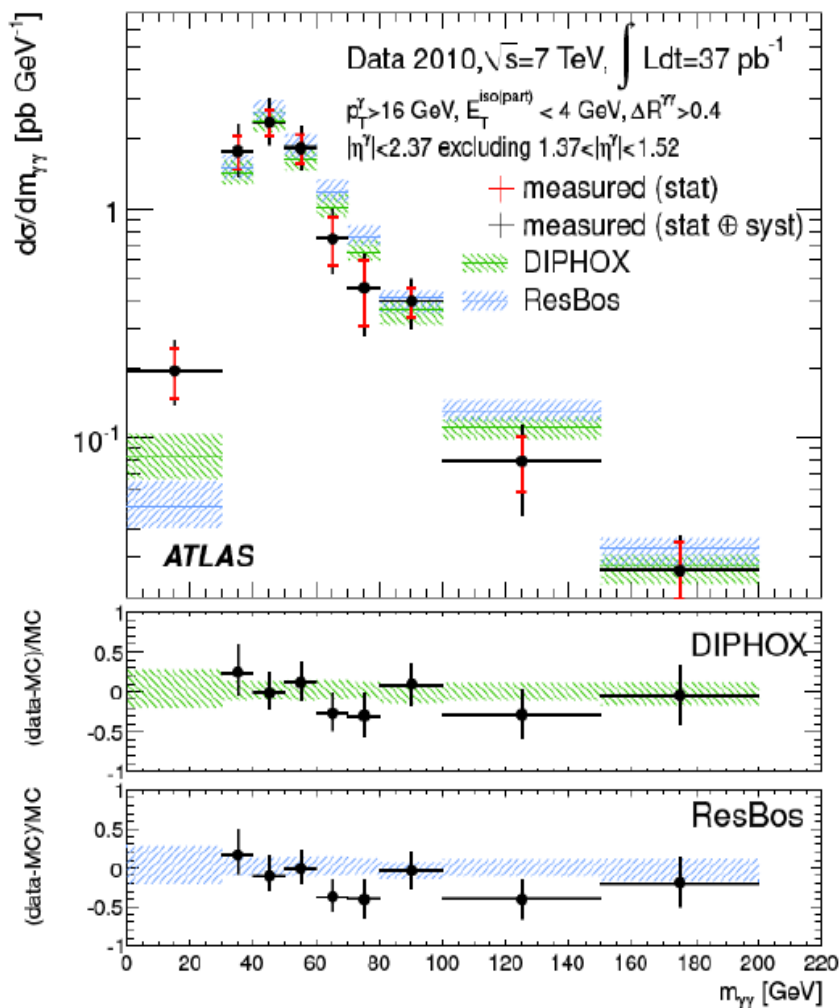


Photon isolation and background estimate

- Background estimated with two methods:
 - ABCD method: extrapolate from the bgd enriched control regions
 - here shown example of 2D template fit



Isolated di-photon cross-section

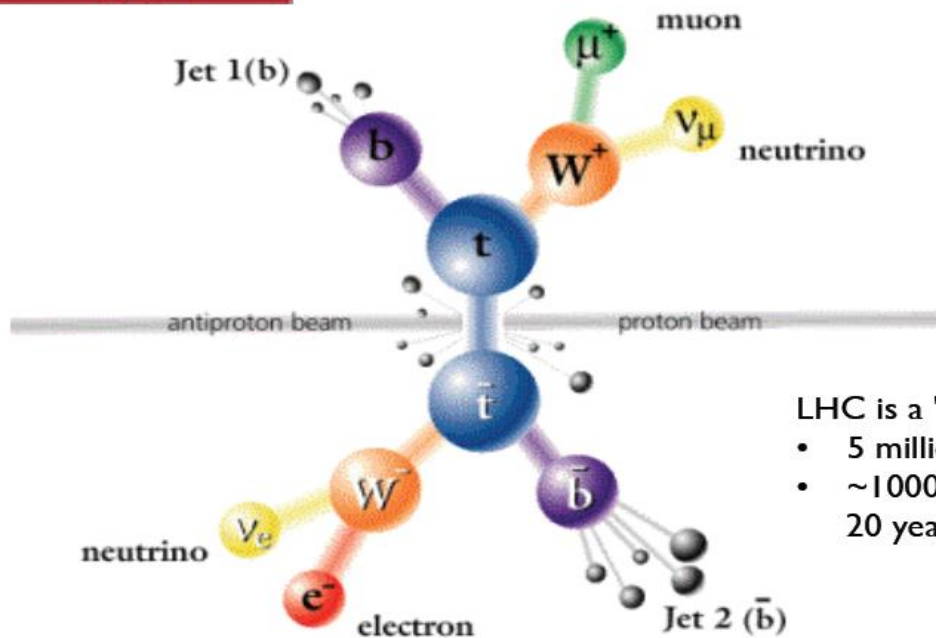
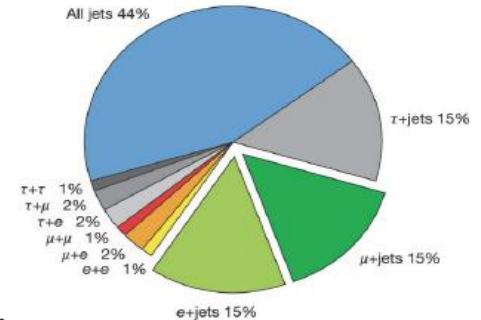


Complicated topologies....

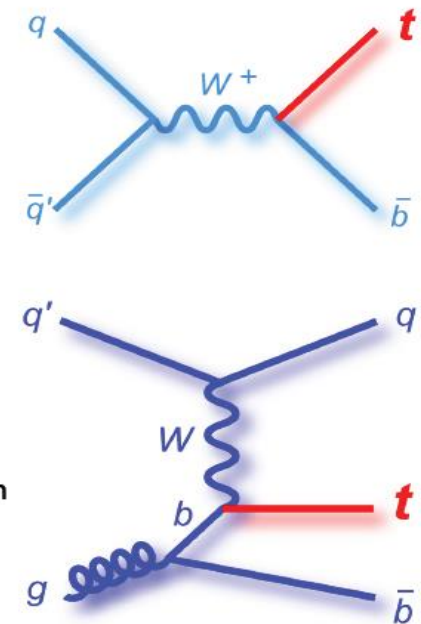
top quark



- Top quark has a mean lifetime of 5×10^{-25} s, shorter than time scale at which QCD acts: no time to hadronize!
 ✓ It decays as $t \rightarrow Wb$
- Events with top quarks are very rich in (b) jets...

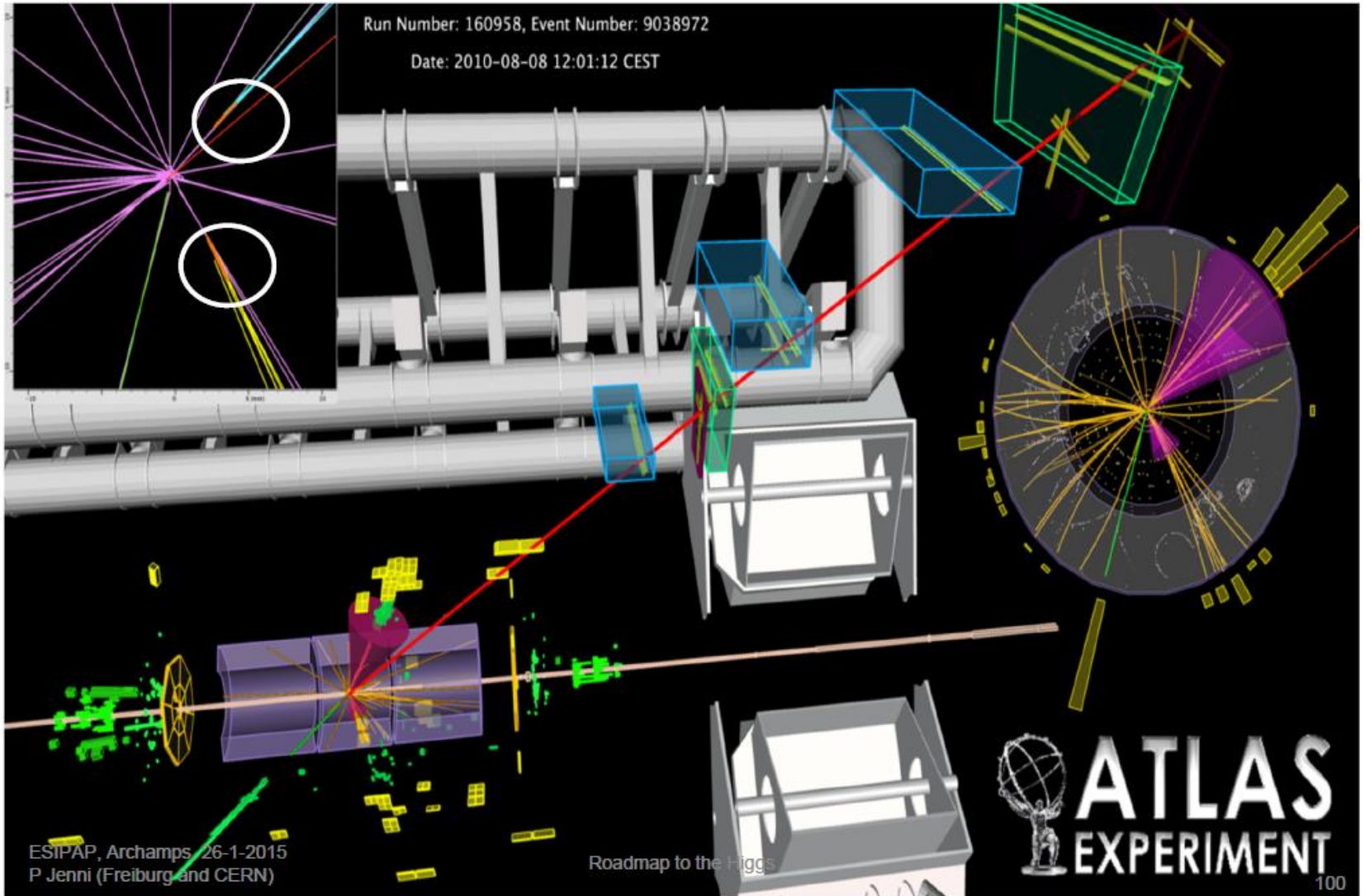


- LHC is a "top factory"!
- 5 millions of $t\bar{t}$ pairs
 - ~ 100000 in Tevatron in 20 years



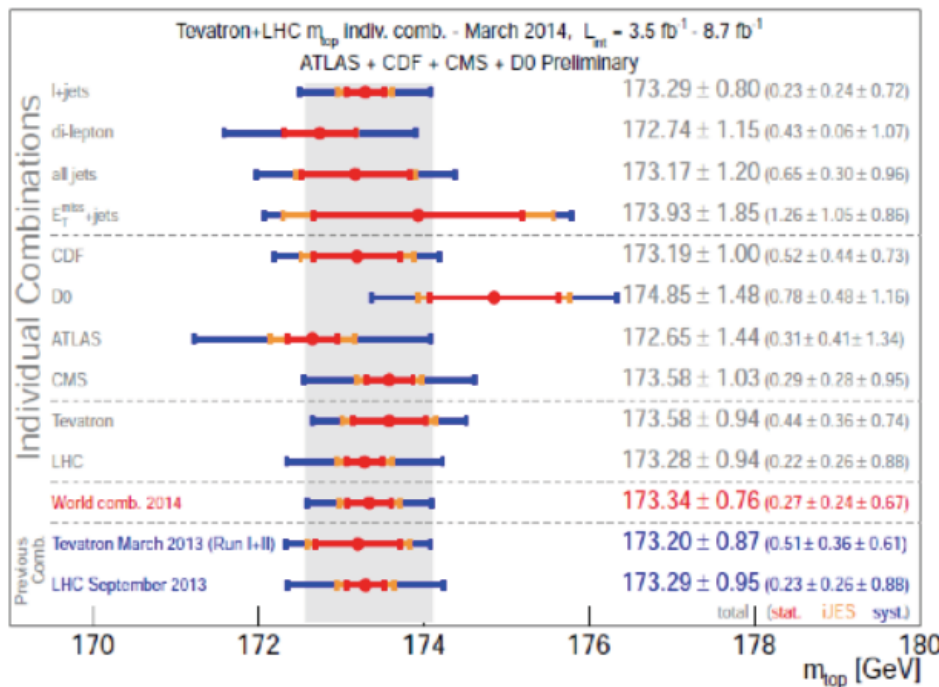
$t\bar{t}$ candidate event

$e + \mu + 2 \text{ jets (b-tagged)} + E_{T\text{miss}}$



Mass of the top quark

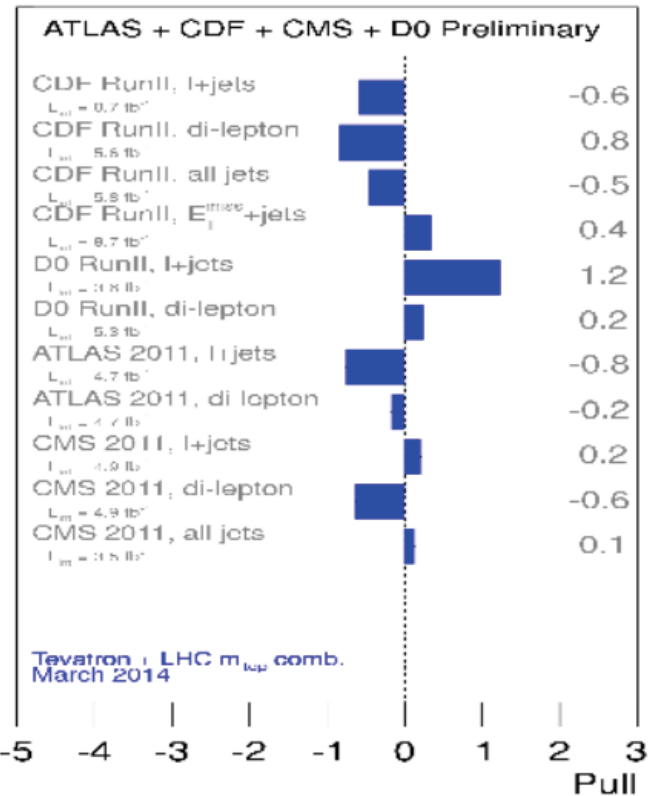
Tevatron combination November 2012 May 2013
 LHC combination July 2012 September 2013
 World combination March 2014 arXiv:1403.4427



$$m_{top} = 173.34 \pm 0.27 \text{ (stat)} \pm 0.24 \text{ (iJES)} \pm 0.67 \text{ (syst)} \text{ GeV}$$

precision on M_{top} 0.44%

Combination using BLUE



Consistency $\chi^2=4/10$

Highest precision in I+jet channel
 Dilepton channel good precision
 Fully hadronic channel respectable ..

Complicated topologies....

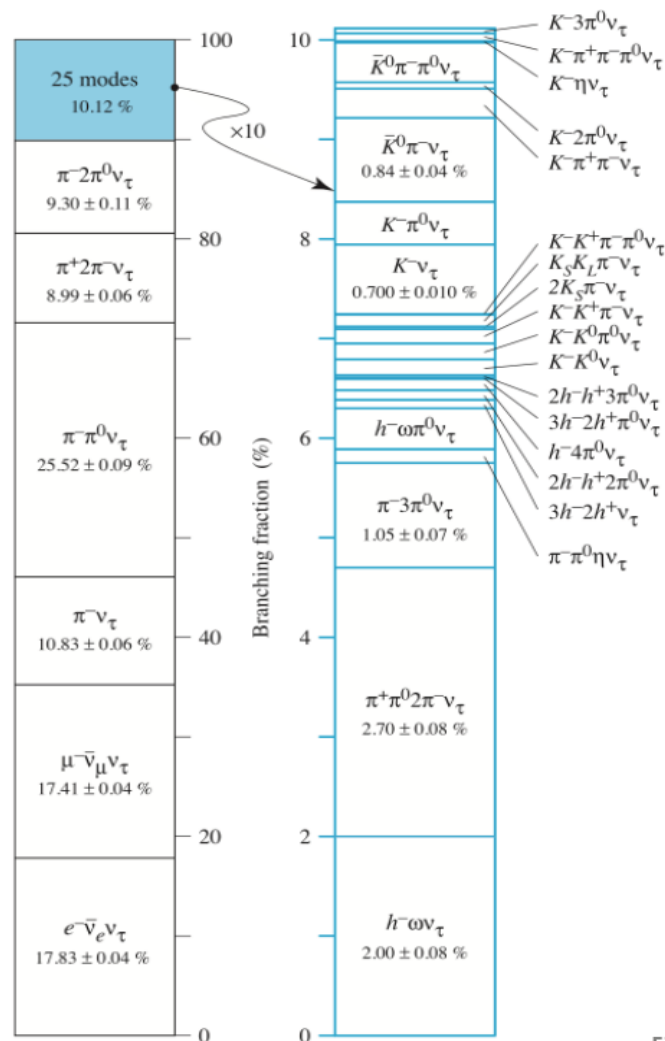
Tau



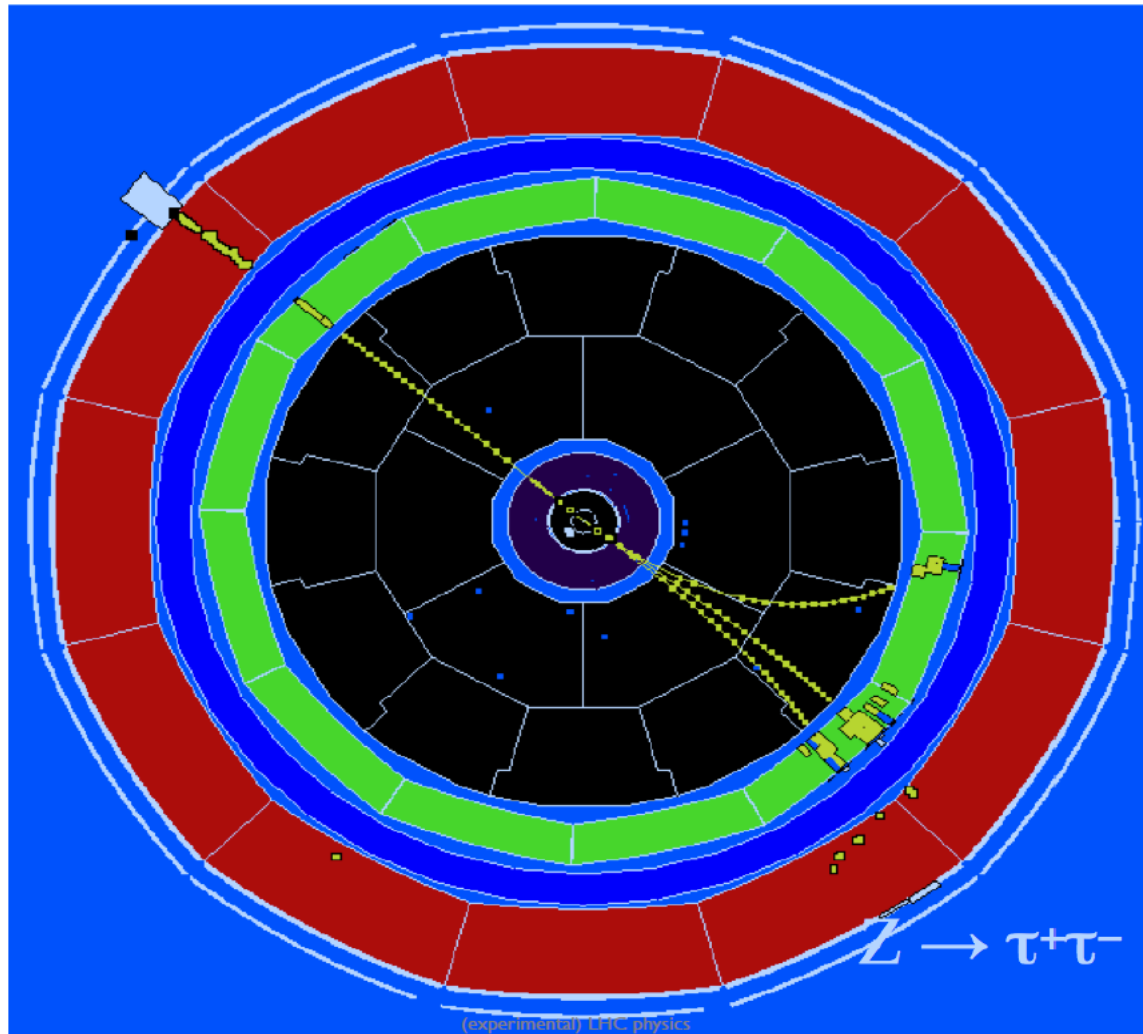
- Tau are heavy enough that they can decay in several final states

- ✓ Several of them with hadrons
- ✓ Sometimes neutral hadrons

- Lifetime = 0.29 ps
 - ✓ 10 GeV tau flies ~ 0.5 mm
 - ✓ Typically too short to be directly seen in the detectors
- Tau needs to be identified by their decay products
- Accurate vertex detectors can detect that they do not come exactly from the interaction point



Complicated topologies....



Electroweak measurements at LHC

Standard Model Production Cross Section Measurements

Status: March 2015

